Tomato brassinosteroid-signaling kinase Bsk830 is a component of flagellin signaling that regulates pre-invasion immunity

Guy Sobol[1], Bharat Bhusan Majhi[1,4], Metsada Pasmanik-Chor[2], Ning Zhang[3], Holly M. Roberts[3], Gregory B. Martin[3], and Guido Sessa[1*]

[1]School of Plant Sciences and Food Security, Tel-Aviv University, 69978 Tel-Aviv, Israel

[2]Bioinformatics Unit, G.S. Wise Faculty of Life Science, Tel-Aviv University, 69978, Tel- Aviv, Israel

[3]Boyce Thompson Institute for Plant Research and Plant Pathology and Plant-Microbe Biology Section, School of Integrative Plant Science, Cornell University, Ithaca, New York 14853, USA

[*]**Correspondence:** Guido Sessa, School of Plant Sciences and Food Security, Tel-Aviv University, 69978 Tel-Aviv, Israel. Email: guidos@tauex.tau.ac.il

[4]**Present Address:** Department of Chemistry, Biochemistry and Physics, Université du Québec à Trois-Rivières, Trois-Rivières, Quebec G9A 5H7, Canada

Running Title: The role of tomato Bsk830 in flagellin signaling

ABSTRACT

Detection of bacterial flagellin by the tomato receptors Flagellin sensing 2 (Fls2) and Fls3 triggers activation of pattern-triggered immunity (PTI). Tomato signaling components associated or downstream of flagellin receptors are largely unknown. We investigated the involvement of tomato brassinosteroid-signaling kinase 830 (Bsk830) in PTI triggered by flagellin perception. Bsk830 localized to the plasma membrane and interacted with Fls2 and Fls3. Consistent with a role in flagellin-induced signaling, CRISPR/Cas9-generated tomato *bsk830* mutants were impaired in ROS accumulation induced by the flagellin-derived flg22 and flgII-28 peptides. In addition, *bsk830* mutants developed larger populations of *Pseudomonas syringae* pv. *tomato* (*Pst*) strain DC3000 than wild-type plants, whereas no differences were observed in plants infected with the flagellin deficient *Pst* DC3000Δ*fliC*. *bsk830* mutants failed to close stomata when infected with *Pst* DC3000 and *Pseudomonas fluorescens,* and were more susceptible to *Pst* DC3000 than wild-type plants when inoculated by dipping, but not by vacuum-infiltration, indicating involvement of Bsk830 in pre-invasion immunity. Analysis of gene expression profiles in *bsk830* mutants detected a reduced number of differentially expressed genes and altered expression of jasmonic acid (JA)-related genes. In support of deregulation of JA response in *bsk830* mutants, these plants were similarly susceptible to *Pst* DC3000 and to the *Pst* DC3118 strain, which is deficient in coronatine production, and more resistant to the necrotrophic fungus *Botrytis cinerea* following PTI activation. These results indicate that tomato Bsk830 is required for a subset of flagellin-triggered PTI responses and support a model in which Bsk830 negatively regulates JA signaling during PTI activation.

INTRODUCTION

Plants have evolved a complex immune system to confront the wide range of pathogens which inhabit their natural environment. Plant immune responses are activated through recognition of highly conserved microbe-associated molecular patterns (MAMPs) by membrane-localized pattern recognition receptors (PRRs) (DeFalco and Zipfel, 2021), or by detection of pathogen effectors by intracellular nucleotide binding leucine-rich repeat receptors (NLR) (Duxbury et al., 2021). In tomato (*Solanum lycopersicum*), known PRRs include Fls2 (Robatzek et al., 2007) and Fls3 (Hind et al., 2016), which perceive the bacterial flagellin-derived peptides flg22 and flgII-28, respectively, and CORE, which detects the bacterial cold shock protein-derived peptide csp22 (Wang et al., 2016). Flg22 and flgII-28 represent major bacterial MAMPs recognized by tomato (Rosli et al., 2013), and their binding by Fls2 and Fls3 activates signaling pathways that regulate molecular events promoting defense, collectively referred to as pattern-triggered immunity (PTI) (Liang and Zhou, 2018). PTI responses include production of reactive oxygen species (ROS), activation of mitogen-activated protein kinases (MAPKs), transcriptional reprogramming, callose deposition at the cell wall, stomatal closure and activation of hormone signaling (DeFalco and Zipfel, 2021).

Stomata closure is a MAMP-triggered and PRR-mediated defense response, also referred to as stomatal immunity, particularly important against leaf-associated pathogenic bacteria, which gain access to the plant apoplast through these natural openings as well as wounds (Melotto et al., 2017). Dynamics of stomatal immunity against phytopathogenic bacteria have been described for the interaction of Arabidopsis and tomato plants with *Pseudomonas syringae* pv. *tomato* (*Pst*) bacteria (Melotto et al., 2006; Du et al., 2014). Plant infection with *Pst* DC3000 causes

stomata closure within 1 h post-inoculation followed by stomata reopening 3-4 h later. Stomatal movement is modulated by ROS accumulation that controls the activity of ion pumps, plasma membrane channels, and transporters (Sierla et al., 2016). In Arabidopsis ROS molecules have been shown to be generated by the NADPH oxidase RBOHD that is activated by phosphorylation upon MAMPs perception by PRRs (Wang and Gou, 2021). MAMP perception also triggers the activation of signaling pathways involving the hormones salicylic acid (SA) and abscisic acid (ABA), which contribute to stomatal closure. Plants defective in SA and ABA synthesis and signaling are unable to induce stomatal closure (Melotto et al., 2017). SA and ABA pathways have been shown to contribute to stomata closure independently and in an interconnected manner (Arnaud and Hwang, 2015).

Stomatal reopening is induced by the pathogen to gain entry into leaves. To promote stomatal reopening, *Pseudomonas syringae* bacteria take advantage of the antagonistic interplay between the plant hormones SA and jasmonic acid (JA) (Thaler et al., 2012). *P. syringae* secretes type III effectors and phytotoxins to enhance JA signaling and repress SA signaling. For example, the HopX1 and HopZ1a effectors induce degradation of JAZ proteins, which are negative regulators of JA signaling, to enhance JA signaling and stomata reopening (Jiang et al., 2013; Gimenez-Ibanez et al., 2014). The *P. syringae* coronatine (COR) phytotoxin is a JA-Ile-mimic molecule that binds the JA receptor COI1 and activates JA-mediated processes (Katsir et al., 2008). Binding of COR to COI1 triggers downstream signaling that induces NAC transcription factors which inhibit SA accumulation and promote stomata reopening (Melotto et al., 2017).

PRRs recruit receptor-like cytoplasmic kinases (RLCKs) to link MAMP perception to downstream signaling. Multiple Arabidopsis RLCKs play a role in plant

immunity. For example, BOTRYTIS-INDUCED KINASE1 (BIK1), a member of the RLCK subfamily VII, associates with multiple PRRs and activates downstream signaling components such as the NADPH oxidase RBOHD (Kadota et al., 2014; Li et al., 2014) and several calcium channels (Tian et al., 2019; Thor et al., 2020). Similar to BIK1, additional members of the RLCK subfamily VII contribute to PTI (Rao et al., 2018). RLCKs regulate stomatal immunity and are essential for the initial closure step (Wang and Gou, 2021). For example, BIK1 and PBL27 regulate stomatal closure by promoting activation of ion channels (Zheng et al., 2018; Liu et al., 2019; Thor et al., 2020).

Brassinosteroid-signaling kinases (BSKs) belong to the RLCK subfamily XII and several of them were extensively characterized in Arabidopsis and shown to play a role in brassinosteroid signaling, growth, and response to abiotic stress (Tang et al., 2008; Li et al., 2012b; Sreeramulu et al., 2013; Jia et al., 2019; Ren et al., 2019). Recent investigation identified Arabidopsis BSKs that are involved in plant immunity (Shi et al., 2013; Majhi et al., 2019 and 2021). BSKs participate in various branches of defense signaling, as evident by their interaction with multiple PRRs, and mediation of different PTI responses. For example, BSK1, BSK5, BSK7, and BSK8 associate with the PRR FLS2 and mutations in the corresponding genes compromise a subset of flg22-mediated PTI responses (Shi et al., 2013; Majhi et al., 2019 and 2021). BSK1 was also found to modulate MAPK activation by phosphorylation of the MAPKKK MAPKKK5 and the MAPK MPK15 (Yan et al., 2018; Shi et al., 2022). In addition, while BSK1, BSK7, and BSK8 interact exclusively with FLS2, BSK5 also interacts with EFR and PEPR1 and is required for their signaling (Majhi et al., 2019). In line with a function of BSKs in immune signaling, *bsk1*, *bsk5*, *bsk7* and *bsk8* mutants display enhanced susceptibility to fungal and bacterial

pathogens (Shi et al., 2013; Majhi et al., 2019 and 2021). Another family member, BSK3, was shown to interact *in vivo* with multiple components of immune signaling (Xu et al., 2014), but its function in plant immunity is yet unknown.

Tomato BSKs are less characterized, but at least two of the seven family members play a role in plant immunity (Singh et al., 2014; Roberts et al., 2019a). A tomato homolog of BSK7 was found to interact with *Pst* DC3000 effectors and silencing of its homologous genes compromised PTI in *Nicotiana benthamiana* (Singh et al., 2014). Tomato Mai1, homolog of Arabidopsis BSK1, interacts with MAPKKKα, a signaling component required for NLR-mediated immunity (Roberts et al., 2019a). Silencing of Mai1 *N. benthamiana* homologs enhanced susceptibility to *Pst* DC3000 and compromised the hypersensitive response mediated by several *R* genes (Roberts et al., 2019a). Here, we investigated the involvement of tomato BSKs in plant immunity. We provide evidence that Bsk830 physically interacts with flagellin receptors and localizes to the cell plasma membrane. Analysis of two independent loss-of-function mutant lines revealed that Bsk830 is required for stomatal immunity against *Pst* DC3000 and for flagellin-induced ROS production. Analysis of gene expression profiles indicated that loss of *Bsk830* caused an attenuated PTI response and deregulation of JA signaling. Consistent with an altered JA response, loss of *Bsk830* compromised the contribution of the COR toxin to *Pst* DC3000 virulence and reduced susceptibility to a fungal necrotrophic pathogen. Together, our results indicate that Bsk830 modulates a subset of flagellin-induced PTI responses and contributes to regulation of JA signaling during PTI.

RESULTS

Tomato Bsk830 interacts with the flagellin receptors Fls2 or Fls3

Recognition of the motility-associated protein flagellin plays a major role in the induction of PTI responses on some tomato accessions (Roberts et al., 2019b). Flagellin contains two MAMPs, flg22 and flgII-28, that are recognized by the PRRs Flagellin sensing 2 (Fls2) and Fls3, respectively (Gómez-Gómez and Boller, 2000; Robatzek et al., 2007; Hind et al., 2016). To investigate the possible involvement of brassinosteroid-signaling kinase (Bsk) proteins in tomato PTI initiated by flagellin perception, we tested interactions of tomato Bsk family members with Fls2 and Fls3 in a yeast two-hybrid system by using Bsk proteins as baits and the kinase domain of Fls2 ($Fls2_{KD}$) and Fls3 ($Fls3_{KD}$) as preys. Bsk830, but none of the other six tomato Bsk family members, interacted with both PRRs (Figure 1A). Next, a split luciferase complementation assay was employed to validate in planta interactions observed in yeast. In these experiments, $Fls2_{KD}$ and $Fls3_{KD}$ were fused to the C-terminal half of the luciferase protein (C-LUC) and co-expressed via *Agrobacterium tumefaciens* in *N. benthamiana* leaves with Bsk830 fused to the N-terminal half of luciferase (N-LUC). As negative controls, C-LUC-PRRs and N-LUC-Bsk830 were co-expressed with N-LUC and C-LUC empty vectors, respectively. Interactions were quantified by measurement of luminescence emitted from leaf discs sampled at 48 h after agro-infiltration. Co-expression of Bsk830 with $Fls2_{KD}$ or $Fls3_{KD}$ resulted in significantly higher luminescence than the negative controls (Figure 1B). Expression in yeast and in planta of all fusion proteins was confirmed by Western blot analysis (Supplemental Figure S1, A and B and Roberts et al., 2019a).

To assess the hypothesis that Bsk830 participates in phosphorylation cascade(s) initiated by Fls2 and Fls3, we tested whether Bsk830 is a substrate of

Fls2 or Fls3 phosphorylation in an *in vitro* kinase assay. Bsk830 and the cytoplasmic domains of Fls2 ($Fls2_{CD}$) and Fls3 ($Fls3_{CD}$) were fused to the C-terminus of the maltose binding protein (MBP), expressed in *E. coli*, and affinity-purified. MBP-$Fls2_{CD}$ and MBP-$Fls3_{CD}$ were incubated with the MBP-BSK830 fusion in the presence of [γ-^{32}P]ATP in an *in vitro* kinase assay. As previously reported (Roberts et al., 2020), MBP-$Fls2_{CD}$ and MBP-$FLS3_{CD}$ displayed autophosphorylation activity (Supplemental Figure S2). However, phosphorylation of MBP-Bsk830 by MBP-$Fls2_{CD}$ or MBP-$Fls3_{CD}$ was not detected (Supplemental Figure S2), indicating that Bsk830 is not a substrate of Fls2 and Fls3 kinase activity *in vitro* despite its interaction with both PRRs.

Lipid modifications anchor Bsk830 to the plasma membrane

The Fls2 and Fls3 PRRs are receptor kinases localized to the plasma membrane (PM) (Andolfo et al., 2013; Hind et al., 2016). Based on the interaction of Bsk830 with Fls2 and Fls3, and the presence of putative myristoylation and palmitoylation sites at the Bsk830 N-terminus (Figure 2A), we hypothesized that Bsk830 is anchored to the PM by fatty acids modifications. To examine this possibility, Bsk830 was fused to the N-terminus of YFP and transiently expressed via *A. tumefaciens* in *N. benthamiana* leaves along with the PM marker Flot1b-mCherry (Li et al., 2012a). Bsk830-YFP displayed a similar distribution as Flot1b-mCherry (Figure 2B, upper panels) that was confirmed by quantifying fluorescence detected in the YFP and mCherry channels along a set path (Figure 2B, lower panels). In contrast to Bsk830-YFP, the Bsk830^{G2A}-YFP and Bsk830$^{C(3,11,12)A}$-YFP variants, which carry mutations in putative myristoylation and palmitoylation sites, respectively, did not co-localize with

Flot1b-mCherry (Figure 2C). These observations suggest that Bsk830 is associated to the PM through myristoylation and palmitoylation modifications.

Mutations in the *Bsk830* gene compromise flagellin-mediated immunity

To investigate the function of Bsk830 in plant immunity, we used CRISPR/Cas9 technology to generate tomato plants with mutations in the *Bsk830* gene. Two independent mutant lines, *bsk830-1* and *bsk830*-2, were generated and allowed to segregate until homozygous genotypes were obtained in the T2 generation. Sequence analysis of the area flanking the gRNA-targeted sequence revealed deletions of 4 bp and 135 bp in the first exon of *Bsk830* in *bsk830-1* and *bsk830-2*, respectively (Supplemental Figure S3). Next, we tested the involvement of Bsk830 in flagellin-induced immunity by examining susceptibility of wild-type and *bsk830* mutant lines to the bacterial pathogen *Pst* DC3000 and its derivative mutant strain *Pst* DC3000Δ*fliC*, which does not form flagella (Kvitko et al., 2009). Plants were inoculated by dipping into suspensions ($1x10^7$ CFU/mL) of *Pst* DC3000 and *Pst* DC3000Δ*fliC*, and bacterial populations were determined in leaf tissue at 2 days post-inoculation (dpi). *Pst* DC3000 bacteria displayed a significantly higher growth in *bsk830* mutant lines than in wild-type plants suggesting that Bsk830 is involved in immunity (Figure 3A). In addition, growth of *Pst* DC3000Δ*fliC* was higher than *Pst* DC3000 in wild-type plants, likely because *Pst* DC3000Δ*fliC*, lacking flagellin, is not detected by Fls2 or Fls3. Conversely, growth of *Pst* DC3000 and *Pst* DC3000Δ*fliC* was similar in the *bsk830* mutants, suggesting that in these plants flagellin-induced immunity is impaired. In line with this conclusion, similar bacterial populations were observed in wild-type plants infected with *Pst* DC3000Δ*fliC* and in *bsk830* mutants infected with *Pst* DC3000 indicating that flagellin-mediated immunity was not

activated in these interactions: in the first instance because the bacteria did not express flagellin, and in the second instance because the plant was impaired in flagellin signaling.

To confirm that *bsk830* mutant plants are impaired in flagellin-induced immunity, we examined PTI responses triggered in these plants by the flg22 and flgII-28 MAMPs. Wild-type and mutant plants were treated with flg22 or flgII-28 and monitored for ROS production and MAPK phosphorylation. The *fls2.1/fls2.2* and *fls3* mutants, which are not responsive to flg22 and flgII-28, respectively (Roberts et al., 2020), were used as negative controls. On treatment with flg22 and flgII-28, *bsk830* mutants accumulated lower levels of ROS than wild-type plants (Figure 3, B and C), while MAPK phosphorylation was similarly activated in both genetic backgrounds (Supplemental Figure S4, A and B). As expected, *fls2.1/fls2.2* and *fls3* mutants did not produce ROS (Figure 3, B and C), and were impaired in the activation of MAPK phosphorylation (Supplemental Figure S4, A and B). Together, these results indicate that Bsk830 is required for a subset of flagellin-induced PTI responses.

Bsk830 mutant plants are impaired in stomatal immunity

In experiments that revealed enhanced susceptibility of *bsk830* mutants to *Pst* DC3000 infection, plant inoculation was carried out by dipping plants into bacterial suspensions. The use of this inoculation technique left unresolved whether Bsk830 is required for immune responses that counteract the pathogen on the leaf surface during the pre-invasion phase of infection or in the leaf apoplast during the post-invasion phase of infection. To differentiate between these possibilities, wild-type plants and *bsk830* mutants were inoculated with a *Pst* DC3000 suspension by vacuum-infiltration ($1x10^5$ CFU/mL), which delivers bacteria directly into the apoplast,

or by dipping ($1x10^7$ CFU/mL), which requires movement of bacteria through stomata for infection. Bacterial populations were determined in leaf tissues sampled at 0 and 2 dpi. *Pst* DC3000 bacteria displayed a significantly higher growth in *bsk830* mutants than in wild-type plants inoculated by dipping (Figure 4A). However, similar bacterial populations were observed in wild-type and mutants plants inoculated by vacuum-infiltration (Figure 4B), suggesting a role for Bsk830 in pre-invasion immunity. A similar stomatal number index was observed for wild-type and *bsk830* mutant plants (Supplemental Figure S5), excluding a bias due to developmental differences between genetic backgrounds used in these experiments.

Because pre-invasion immunity relies on stomatal closure to prevent entrance of bacteria into the leaf apoplast (Melotto et al., 2017), we examined dynamics of stomatal opening/closure in *bsk830* mutants upon infection with *Pst* DC3000 pathogenic bacteria and *Pseudomonas fluorescens* (*Pf*) A506 non-pathogenic bacteria. Both types of bacteria are known to induce stomatal closure early after infection, but only pathogenic bacteria overcome this line of defense at later stages of infection by using virulence factors to reopen stomata (Melotto et al., 2017). Prior to bacterial challenge, leaf pieces of wild-type and *bsk830* mutant plants were floated on stomatal opening buffer under light to ensure stomata opening. After 3 h, leaf pieces were transferred to *Pst* DC3000 or *Pf* bacterial suspension ($1x10^8$ CFU/mL), or kept on buffer (mock), and monitored for stomatal apertures during the following 4 h. At 0 h, stomata of both plant genotypes were similarly open, suggesting that loss of function in *Bsk830* does not interfere with light-induced stomatal opening (Figure 4, C and D). On *Pst* DC3000 treatment, stomata of wild-type plants closed at 1 h after infection and reopened at 2.5 h (Figure 4C), while on *Pf* treatment, they closed at 2.5 h and remained closed at 4 h (Figure 4D). In contrast, on both treatments,

stomata of the *bsk830* mutant plants remained open for the entire course of the experiment similar to mock-treated plants (Figure 4, C and D). These results indicate that Bsk830 is required for stomatal closure associated with pre-invasion immunity.

Loss of function in *Bsk830* alters expression of JA- and phenylpropanoid-related genes during PTI

To uncover molecular mechanisms underlying the contribution of Bsk830 to tomato immunity, we compared expression profiles of wild-type and *bsk830* mutant plants during the onset of PTI. Leaves of wild-type and *bsk830-1* lines were inoculated by vacuum-infiltration with a suspension ($1x10^8$ CFU/mL) of *Pf* bacteria or a mock solution; samples were collected at 0 and 6 h post-inoculation, and subjected to RNA-seq analysis. In these experiments, we opted for induction of PTI by non-pathogenic rather than by pathogenic bacteria to avoid possible interference of virulence factors. In addition, plants were inoculated by vacuum-infiltration, rather than by dipping, to assure an equal bacterial load in the inoculated leaves despite the defective dynamics of stomatal closure of *bsk830* mutants. A total of 2,146 (852 up-regulated; 1,294 down-regulated) and 1,325 (655 up-regulated; 665 down-regulated) differentially expressed genes (DEGs) were identified in *Pf*- inoculated wild-type and *bsk830* mutant plants, respectively, as compared to mock inoculated plants with filtering parameters of pFDR < 0.05 and a fold change >3 (Figure 5A; Supplemental Table S1). 1,207 DEGs were common to both genotypes, whereas 939 and 118 were unique to wild-type and *bsk830* mutant plants, respectively (Figure 5A). These results suggest that *bsk830* mutants were less responsive to *Pf* inoculation than wild-type plants.

To identify cellular processes in which Bsk830 is involved, we examined functional categories over-represented among genes that were expressed in wild-type plants, but not in the *bsk830* mutant or vice versa, and genes whose fold-change during PTI differed by at least ±20% between the *bsk830* mutant and the wild-type. Arabidopsis homologs of genes from this pool were subjected to functional enrichment analysis by using the g:Profiler tool (Raudvere et al., 2019) as separate entries based on their up- or down-regulation during PTI. The use of Arabidopsis homologs allowed a more extensive characterization of the gene pool in comparison to the use of tomato gene accessions. Among genes up-regulated during PTI, the predominant functional categories enriched in the *bsk830* mutant were related to JA signaling and response, and to metabolism of phenylpropanoids (Table 1). In *bsk830* mutant, expression of genes involved in JA biosynthesis (e.g., AOS, LOX3, OPR2; Wasternack and Song, 2016), catabolism (e.g., JAO2, JAO3, CYP94B1; Smirnova et al., 2017), and negative regulation of JA signaling (e.g., JAZ2, JAZ3, JAZ7, JAZ9, JAM2; Sasaki-Sekimoto et al., 2013) was reduced as compared to wild-type plants (Figure 5B, Supplemental Table S1). In addition, the transcript abundance of genes encoding various JA response factors (e.g., NATA1, TD, PI-I, ERF1, ERF5, JA2L; Du et al., 2017) was reduced or increased (Figure 5B, Supplemental Table S1). Genes related to phenylpropanoid metabolism displayed increased expression in the *bsk830* mutant and included homologs of phenylalanine ammonia-lyase (PAL) as well as enzymes acting downstream to PALs and involved in lignin biosynthesis (Vanholme et al., 2019) (Supplemental Table S1). Among genes down-regulated during PTI, the predominant categories enriched in the *bsk830* mutant were mainly related to photosynthesis (Table 1). Expression of photosynthesis-related genes was more elevated in the *bsk830* mutant than in wild-type plants (Supplemental Table S1),

316 suggesting a less extensive reallocation of resources from general metabolism to
317 defense that is usually observed in plants activating immune responses (Attaran et
318 al., 2014). Together, these results suggest that loss of *Bsk830* results in a weaker
319 PTI response and altered regulation of JA signaling and response.
320
321 **Mutation of *Bsk830* affects JA-mediated phenotypes**
322 To assess the hypothesis that loss of *Bsk830* causes altered regulation of the JA
323 response during the onset of PTI, we examined the contribution of the COR toxin to
324 *Pst* DC3000 virulence in wild-type and *bsk830* mutant plants. COR is a hormone
325 mimic, which closely resembles JA-Ile (Katsir et al., 2008), and it has been shown to
326 activate JA signaling and promote stomatal opening (Melotto et al., 2017). Leaves of
327 wild-type, *bsk830-1* and *bsk830-2* lines were inoculated by dipping in bacterial
328 suspensions ($1x10^7$ CFU/mL) of *Pst* DC3000 (able to synthesize COR; COR+) or *Pst*
329 DC3118 (unable to synthesize COR; COR-), and bacterial populations were
330 determined in leaves at 0 and 2 dpi. In wild-type plants, *Pst* DC3000 (COR+)
331 bacteria displayed a significantly higher growth than *Pst* DC3118 (COR-) (Figure 6A)
332 indicating that COR promotes bacterial virulence, as previously reported (Zheng et
333 al., 2012; Du et al., 2014; Gimenez-Ibanez et al., 2017). Conversely, in *bsk830*
334 mutant plants, *Pst* DC3000 (COR+) and *Pst* DC3118 (COR-) displayed a similar
335 growth indicating that mutation of *Bsk830* compromises the contribution of COR to
336 bacterial virulence and suggesting that, similar to COR, a mutation in *Bsk830*
337 deregulates the JA response.
338 Next, we examined the effect of loss of function in *Bsk830* on susceptibility to
339 the necrotrophic fungal pathogen *Botrytis cinerea*, which is known to be mediated by
340 JA (Zhang et al., 2017). Wild-type and *bsk830* mutant plants were pretreated with a

mock solution or with a *Pf* bacterial suspension ($1x10^8$ CFU/mL) to activate PTI, and 24 h later plants were infected by placing on the leaves a droplet of a *B. cinerea* spore suspension (2×10^5 conidia mL^{-1}). Lesion diameter in infected leaves was measured at 3 dpi (Figure 6B). Wild-type and *bsk830* mutant plants were equally susceptible to *B. cinerea* when mock treated. However, following the *Pf* treatment, symptoms developed more slowly and lesions were significantly smaller in leaves of *bsk830* mutant plants than in wild-type plants. These results support a model in which the JA response is deregulated during the onset of PTI in *bsk830* mutant plants.

DISCUSSION

We identified the tomato RLCK Bsk830 as a component of signaling pathways originated from perception of bacterial flagellin by the Fls2 and Fls3 PRRs. Initial indication for the involvement of Bsk830 in plant immunity was its interaction with the flagellin receptors Fls2 and Fls3 that was observed in yeast and then validated in planta. Subsequent analysis of *bsk830* mutant plants revealed that Bsk830 is required for pre-invasion immunity by mediating a subset of PTI responses including ROS accumulation and stomatal closure possibly through negative regulation of JA signaling. BSK family members appear to play a role in flagellin-induced signaling in different plant species: in tomato, Bsk830 (but not other Bsk family members) is recruited by two flagellin receptors and is required for flagellin-induced immunity, while in Arabidopsis multiple BSKs (BSK1, BSK5, BSK7, BSK8) interact with the FLS2 PRR and play a role in flg22-induced PTI (Shi et al., 2013; Majhi et al., 2019 and 2021). It remains to be determined whether Bsk830 participates only in signaling pathways activated by flagellin-derived MAMPs, similar to its closest Arabidopsis homologs BSK7 and BSK8 (required for PTI responses triggered by flg22, but not by elf18 and pep1 [Majhi et al., 2021]), or if it is involved in signaling events activated by multiple MAMPs, as observed for Arabidopsis BSK5 (Majhi et al., 2019).

Similar to other BSK family members (Majhi et al., 2019 and 2021; Ren et al., 2019; Roberts et al., 2019a; Su et al., 2021), Bsk830 localizes to the plasma membrane, where it may interact with PRRs and associated components of immune complexes. N-terminal sites predicted to mediate myristoylation and palmitoylation modifications were essential to its plasma membrane localization, common mechanisms used by BSKs for plasma membrane anchoring (Majhi et al., 2019 and 2021; Ren et al., 2019; Roberts et al., 2019a; Su et al., 2022) or maintenance of

protein stability, as demonstrated for BSK1 (Su et al., 2022). However, the output of the interaction of Bsk830 with Fls2 and Fls3 is yet unknown. It is unlikely that Bsk830 is activated by Fls2 and/or Fls3 phosphorylation, because Fls2 and Fls3 were not able to phosphorylate Bsk830 *in vitro* despite detection of their autophosphorylation activity. It is possible that additional molecules, which participate *in vivo* in Bsk830 phosphorylation by Fls2 and Fls3, are missing *in vitro*. Alternatively, Bsk830 might function as a scaffolding protein that mediates signal transduction by bringing signaling components in proximity, as it has been suggested for other BSKs (Sreeramulu et al., 2013; Ren et al., 2019; Majhi et al., 2019 and 2021). The latter hypothesis is supported by the evidence that Bsk830 autophosphorylation was not detected under the conditions used in our *in vitro* experiments.

Phenotypic analysis of *bsk830* mutant lines revealed that Bsk830 is required for a subset of PTI responses induced by flagellin-derived MAMPs, including ROS production, but not MAPK phosphorylation. This result, together with previous observations that Arabidopsis *bsk1*, *bsk5*, *bsk7* and *bsk8* mutant lines are impaired in flg22-induced ROS production (Shi et al., 2013; Majhi et al., 2019 and 2021), confirms a central role of BSK family members in signaling pathway(s) that link flg22 sensing to ROS accumulation. Conversely, it is less likely that BSK family members are involved in signaling of flg22-induced MAP kinase activation. In our experiments, a mutation in *Bsk830* did not alter MAP kinase activation induced by flg22 treatment in tomato plants. Similarly, Arabidopsis lines carrying different combinations of mutations in *BSK* genes, including up to seven *BSK*s, displayed a similar MAPK activation as wild-type plants following flg22 challenge (Majhi et al., 2021). However, it is still possible that BSKs participate in MAP kinase activation induced by other MAMPs or pathogen effectors. In support of this hypothesis, BSK1 was shown to

400 phosphorylate *in vitro* MAPKKK5 and MPK15, and required for disease resistance
401 mediated by these MAPKKKs against virulent and avirulent *Pst* DC3000 strains and
402 powdery mildew fungi, respectively (Yan et al., 2018; Shi et al., 2022).
403 We provide evidence that Bsk830 is involved in pre-invasion immunity, as *bsk830*
404 mutants failed to close stomata when inoculated with pathogenic and non-
405 pathogenic bacterial strains, and displayed enhanced susceptibility to *Pst* DC3000
406 when inoculated by dipping, but not by vacuum-infiltration. Stomata closure is a PTI
407 response that prevents bacteria from entering the plant apoplast and is activated by
408 detection of MAMPs by PRRs (Melotto et al., 2017). For example, Arabidopsis plants
409 mutated in FLS2 or in both PEPR1 and PEPR2 PRRs fail to close stomata when
410 challenged with the respective MAMPs, and are more susceptible to *Pst* DC3000
411 when dip-inoculated, but not when syringe-infiltrated (Zipfel et al., 2004; Melotto et
412 al., 2006; Zheng et al., 2018). In Arabidopsis, the RLCKs BIK1 and PBL27 act
413 downstream of PRRs in signaling pathways that lead to stomata closure (Wang and
414 Gou, 2021). BIK1 transduces the signal generated by recognition of flg22 and pep1
415 by their respective PRRs and activates anion channels that cause stomata closure
416 (Kadota et al., 2014; Li et al., 2014; Guzel Deger et al., 2015; Zheng et al., 2018;
417 Thor et al., 2020). Similarly, PBL27, interacts with the chitin receptor CERK1 and
418 upon chitin elicitation activates anion channels that cause stomata closure (Liu et al.,
419 2019). RLCKs of the BSK subfamily were not examined in the context of stomatal
420 movement, with the exception of the observation that *BSK5* mutant plants are
421 hypersensitive to ABA in stomatal closure (Li et al., 2012b).
422 Comparison of gene expression profiles of *bsk830* mutant and wild-type tomato
423 plants during the activation of PTI allowed us to formulate hypotheses about the
424 molecular mechanisms of Bsk830 to regulate PTI responses. A prominent difference

425 between *bsk830* mutants and wild-type plants was differential expression of genes
426 related to JA biosynthesis, catabolism, signaling, and response. JA regulates
427 stomatal aperture by promoting their opening, as opposed to SA that promotes
428 stomata closure in response to bacterial pathogens in Arabidopsis and tomato plants
429 (Lee et al., 2013; Melotto et al., 2017; Guzman et al., 2020). Pathogens manipulate
430 stomata aperture by secretion of JA mimicking molecules or effectors (Melotto et al.,
431 2017). For example, *Pst* DC3000 secretes COR, a hormone mimic that closely
432 resembles JA-Ile, that promotes degradation of JAZ proteins which negatively
433 regulate transcription of JA-related genes and signaling (Zhang et al., 2017).
434 Activation of the JA pathway leads to an inhibitory effect on accumulation of salicylic
435 acid, which in turn promotes stomatal reopening (Melotto et al., 2017). Our
436 expression profiles data indicates a release of negative regulation of JA signaling in
437 the *bsk830* mutants compared to wild-type plants. This was confirmed by the lack of
438 COR contribution to *Pst* DC3000 virulence in *bsk830* mutants, and their increased
439 resistance to a fungal necrotrophic pathogen following PTI activation (Zhang et al.,
440 2017). We therefore propose a model in which Bsk830 negatively regulates JA
441 signaling and response that promote stomatal closure and ROS production (Yi et al.,
442 2014; Toum et al., 2016). This is reminiscent of other regulators of plant immunity,
443 such as FERONIA, which destabilizes MYC2, a regulator of JA signaling, to inhibit
444 COR-induced signaling and promote disease resistance (Guo et al., 2018), and
445 LINC1, which negatively regulates transcription of JA-related genes to enhance PTI
446 (Jarad et al., 2020). In conclusion, our data reveal an important role for tomato
447 Bsk830 in pre-invasion immunity initiated by flagellin perception and in regulation of
448 JA signaling and response during PTI.

MATERIALS AND METHODS

Plant materials and growth

Plant cultivars used were: *Nicotiana benthamiana* (Goodin et al., 2008), and tomato (*Solanum lycopersicum*) Hawaii 7981 (Wang et al., 2011). *N. benthamiana* plants were grown in a phytochamber at 25°C in long-day conditions (16 h/8 h, light/dark). Tomato plants were grown in a greenhouse with temperatures fluctuating between 25°C to 30°C under natural light conditions.

Strains and growth conditions of bacteria, fungi, and yeast

The strains used were: *Escherichia coli* DH5α (Invitrogen) and Rosetta (MERCK), *Pseudomonas syringae* pv. *tomato* (*Pst*) DC3000 (Guo et al., 2009), *Pst* DC3000Δ*fliC* (Kvitko et al., 2009), *Pst* DC3118 (Ma et al., 1991), *Pseudomonas fluorescens* A506 (Wilson et al., 2002), *Agrobacterium tumefaciens* GV2260 (Deblaere et al., 1985) and LBA4404 (Ooms et al., 1982), *Botrytis cinerea* B05.10 (Ma et al., 2017), and yeast (*Saccharomyces cerevisiae*) Y2HGold (Clontech). Bacterial, fungal, and yeast strains were grown with the appropriate antibiotics as follows: *E. coli* in Lysogeny broth (LB) medium at 37°C; *Pst*, *Pf*, and *A. tumefaciens* in LB at 30°C; *B. cinerea* in potato dextrose broth at 20°C; yeast in synthetically defined medium (6.7 g/L yeast nitrogen base without amino acids, 1.4 g/L amino acid drop-out mix) supplemented with 2% (w/v) glucose at 30°C.

Pathogenicity assays

Tomato plants were inoculated by vacuum-infiltration with bacterial suspensions of $1x10^5$ CFU/mL in 10 mM $MgCl_2$ and 0.008% (v/v) Silwet L-77 (apart from *Pf* A506, which was inoculated at a concentration of $1x10^8$ CFU/mL), or by dipping into

474 bacterial suspensions of $1x10^7$ CFU/mL in 10 mM $MgCl_2$ and 0.04% Silwet L-77.
475 Plants inoculated by dipping were placed in a sealed transparent box to maintain
476 humidity. Leaflets were with 3% (w/v) bleach, rinsed with water, and dried. Five
477 samples of four leaf discs (1 cm diameter) were taken from three plants at 2 h after
478 inoculation (day 0) and 2 days later, and homogenized in 1 mL of 10 mM $MgCl_2$ to
479 determine bacterial populations via serial dilution plating.
480 For tomato inoculation with *Botrytis cinerea,* droplets (7 µL) of 0.5X potato dextrose
481 broth containing $2x10^5$ spores/mL were deposited on the leaf surface. The area of
482 disease lesions was measured three days after inoculation.
483
484 **Peptide elicitors**
485 Peptides flg22 (QRLSTGSRINSAKDDAAGLQIA; Krol et al., 2010) and flgII-28
486 (ESTNILQRMRELAVQSRNDSNSSTDRDA; Clarke et al., 2013) were purchased
487 from Integrated DNA Technologies, Inc., dissolved in water to a 5 mM stock solution,
488 and diluted to the working concentration.
489
490 ***A. tumefaciens*-mediated transient expression**
491 Overnight cultures of *A. tumefaciens* were pelleted, washed three times with 10 mM
492 $MgCl_2$, resuspended in induction medium (10 mM $MgCl_2$, 10 mM MES [pH 5.6], and
493 200 µM acetosyringone), and incubated with shaking for 3-4 h at 20°C. Cultures
494 were diluted to OD_{600}=0.2 and infiltrated into leaves of *N. benthamiana* plants using a
495 needleless syringe.
496
497 **Generation of CRISPR/Cas9-mediated knockout lines**

To generate tomato lines with mutations in the *Bsk830* gene, guide RNAs (gRNA1: GATTCTGAGCCTCGTGAATG; gRNA2: GTTTAACAGCAACCGGCCTC) targeting the first exon of *Bsk830* were designed using the tomato genome version SL2.5 (Tomato Genome Consortium, 2012) and the Geneious R11 software (https://www.geneious.com). Each gRNA was cloned into a Cas9-expressing binary vector (p201N:Cas9; Jacobs et al., 2015) by Gibson assembly (Jacobs et al., 2017) and transformed into *A. tumefaciens* LBA4404. The obtained strains were pooled and used to transform Hawaii 7981 tomato plants at the Boyce Thompson Institute transformation facility (Frary and Van Eck, 2005). To determine the mutation type, genomic DNA was extracted from transgenic leaves using a modified CTAB method (Murray and Thompson, 1980). Genomic regions flanking the target site of the *Bsk830* gene were amplified with primers 15-16 (Supplemental Table S2) and sequenced.

Yeast two-hybrid assay

A GAL4 two-hybrid system was used to analyze protein-protein interactions in yeast. pGBKT7 vectors (bait) carrying tomato Bsk family members fused to the GAL4 DNA binding domain were as described (Roberts et al., 2019a). Gene fragments encoding the kinase domains of Fls2 ($Fls2_{KD}$; amino acids 867 to 1,169) or Fls3 ($Fls3_{KD}$; amino acids 854 to 1,140) were PCR-amplified from tomato cDNA using primers 3-4 ($Fls2_{KD}$) or 1-2 ($Fls3_{KD}$) (Supplemental Table S2) and fused to the GAL4 activation domain in the pGADT7RecM vector (prey). Interactions were tested by placing droplets of yeast (10 µl) carrying bait and prey vectors on SD medium lacking Leu and Trp (SD−LW), SD−LW lacking His and adenine (SD-LWHA), or SD−LW supplemented with 25 µg/ml Aureobasidin A (SD–LW+AbA).

523

524 **Split luciferase complementation assay**

525 Gene fragments encoding $Fls2_{KD}$ and $Fls3_{KD}$ were PCR-amplified from tomato cDNA
526 using primers 7-8 ($Fls2_{KD}$) or 5-6 ($Fls3_{KD}$) (Supplemental Table S2), and cloned in
527 frame to the C-terminal fragment of firefly luciferase in the binary vector
528 pCAMBIA1300:C-LUC (Chen et al., 2008). Bsk830 was cloned in frame to the N-
529 terminal fragment of firefly luciferase in the binary vector pCAMBIA1300:N-LUC
530 (Chen et al., 2008), as described (Roberts et al., 2019a). The obtained vectors were
531 transformed into *A. tumefaciens* GV2260 and co-expressed in *N. benthamiana*
532 leaves. Split luciferase complementation assays were performed as described (Majhi
533 et al., 2019).

534

535 **Subcellular localization**

536 Gene fragments encoding *Bsk830*, $Bsk830^{G2A}$, and $Bsk830^{C(3,11,12)A}$ were PCR-
537 amplified from tomato cDNA using primers 9-10, 11-10, and 12-10, respectively
538 (Supplemental Table S2). Amplified fragments were fused upstream of the coding
539 region of the yellow fluorescence protein (YFP) in the pBTEX binary vector driven by
540 the CaMV 35S promoter (Frederick et al., 1998; Popov et al., 2016). Fusion proteins
541 were co-expressed with the plasma membrane marker Flot1b-mCherry (Li et al.,
542 2012a) via *A. tumefaciens* GV2260 in *N. benthamiana* leaves and their localization
543 was visualized by a Zeiss LSM780 confocal laser scanning microscope (Zeiss). YFP
544 was excited with an argon laser at 514 nm, while mCherry and mRFP were excited
545 with a DPSS561-10 laser at 561 nm. Emission was detected between 518 and 583
546 nm for YFP, and between 579 and 650 nm for mCherry and mRFP. Images were
547 processed with the image processing package Fiji (https://fiji.sc/).

548

549 **Expression of MBP fusion proteins in *E. coli* and *in vitro* kinase assay**

550 A gene fragment encoding Bsk830 was PCR-amplified from tomato cDNA using
551 primers 13-14 (Supplemental Table S2), and cloned into the pMAL-c2x vector (New
552 England Biolabs). $Fls2_{CD}$ (amino acids 841 to 1,169), and $Fls3_{CD}$ (amino acids 824 to
553 1,140) MBP fusions in the pMAL-c2x vector were prepared as described (Roberts et
554 al., 2020). Proteins were expressed in the Rosetta *E. coli* strain and purified (Majhi et
555 al., 2019). MBP fusion proteins were incubated at 25°C for 1 h in a kinase assay
556 solution containing 50 mM Tris-HCl (pH 7), 1 mM DTT, 10 mM $MgCl_2$, 10 mM $MnCl_2$,
557 20 µM ATP, and 10 µCi [γ-^{32}P]ATP (3,000 Ci mmol^{-1}; Perkin-Elmer). Reactions were
558 stopped by addition of the SDS sample buffer. Half of the reaction was fractionated
559 by SDS-PAGE and stained with Coomassie Blue. The second half was fractionated
560 by SDS-PAGE, blotted onto a PVDF membrane and exposed to autoradiography.

561

562 **Protein extraction**

563 Protein extraction from yeast and leaves was performed as described by Salomon
564 and Sessa (2010) and Majhi et al. (2019), respectively.

565

566 **ROS production assay**

567 Leaf discs were placed in 200 µL of water overnight with the adaxial side up in 96-
568 well plates. The next day, the water was replaced with a solution containing 100 nM
569 flg22 or flgII-28, 34 µg mL^{-1} luminol (Sigma-Aldrich), and 20 µg mL^{-1} horseradish
570 peroxidase (Sigma-Aldrich). Luminescence was measured with a Veritas Microplate
571 Luminometer (Turnerbiosystems Veritas) for 30 min (flg22) or 45 min (flgII-28) at 2.5-
572 or 3-min intervals, with a reading time of 2 sec per well.

573

574 **MAPK phosphorylation assay**

575 Leaf discs (~60 mg) were floated overnight in 10 mL water in 6-well-plates and then
576 treated with 1 µM flg22, 1 µM flgII-28, or water. Total proteins were extracted in 150
577 µL extraction buffer (50 mM Tris-HCl [pH 7.5], 200 mM NaCl, 1 mM EDTA, 10 mM
578 NaF, 1 mM Na_2MoO_4, 2 mM Na_3VO_4, 10% [v/v] glycerol, 2 mM DTT, and 1 mM
579 PMSF). Proteins were fractionated by SDS-PAGE, transferred onto PDVF
580 membranes, and immunoblotted with rabbit anti-pMAPK antibodies (α-pMAPK; Cell
581 Signaling Technology).

582

583 **Measurements of stomatal aperture and number**

584 Leaf pieces were cut from tomato leaflets and floated on stomatal buffer (25 mM
585 MES-KOH [pH 6.15] and 10 mM KCl) for 3 h under light to allow stomata to fully
586 open (Melotto et al., 2006; Guzman et al., 2020). Leaf pieces were then floated on
587 water (control) and suspensions ($1x10^8$ CFU/mL) of *Pst* DC3000 or *Pf* A506. At the
588 indicated times, leaf pieces were removed, dried with a filter paper, and placed on an
589 Elite HD+ silicon rubber mixture (Zhermack) to create an impression of the leaf
590 abaxial surface (Weyers and Johansen, 1985). Once hardened, the silicone rubber
591 mixture was covered with clear nail varnish, which was allowed to dry, transferred to
592 a glass slide, and observed under an Axio Zoom.V16 microscope (Zeiss). For each
593 data point, the width and length of approximately 100-200 stomatal apertures were
594 measured by using the Fiji package (https://fiji.sc/) and used to calculate the
595 Stomatal Aperture Index. Images were also used to calculate the Stomata Number
596 Index (Zhang et al., 2020).

597

598 **RNA-seq cDNA library preparation**

599 Total RNA was isolated with the RNeasy Plant Mini Kit (QIAGEN) from wild-type and
600 *bsk830-1* tomato leaves inoculated by vacuum with *P. fluorescens* A506 or mock-
601 inoculated (three biological replicates for treatment, in total 12 samples collected at 6
602 h post-inoculation). RNA integrity was evaluated using the 4200 TapeStation System
603 (Agilent Technologies). RNA-Seq cDNA libraries were prepared from RNA samples
604 using the NEBNext Ultra™ II mRNA Library Prep Kit for Illumina and then PCR-
605 amplified using NEBNext Multiplex Oligos for Illumina (New England Biolabs).
606 Quality and average size of cDNAs in the library were evaluated using the 4200
607 TapeStation System (Agilent Technologies).
608
609 **Next-generation sequencing and data analysis**
610 Libraries were sequenced using a NextSeq™ 500 system (Illumina) at the Genomics
611 Research Unit of the Faculty of Life Sciences, Tel Aviv University. FASTQ files
612 obtained from the sequencing were analyzed by Partek® Flow® 8.0 using the
613 *Solanum lycopersicum* SL3.0 assembly (NCBI ID 393272). Raw reads with Phred
614 quality scores of less than 20 were trimmed from the 3′ end, followed by removal of
615 adaptor sequences. High quality trimmed reads (Phred score ~34 and read length 75
616 bp) were aligned to the reference genome by STAR 2.7.3a (Dobin et al., 2013).
617 Gene expression quantification was performed using the Partek E/M algorithm (Xing
618 et al., 2006), and normalized to RPKM (reads per kilobase of transcript per million
619 mapped reads) (Mortazavi et al., 2008). Gene-specific analysis was performed on
620 15,575 detected genes (false discovery rate [pFDR] < 0.05). Overlap of differentially
621 expressed genes in wild-type and *bsk830-1* plants was visualized using the eulerr R
622 package (Larsson, 2020). Gene ontology (GO) enrichment analysis was performed

using g:Profiler (version e105_eg52_p16_e84549f) with a significance threshold of pFDR < 0.05 (Raudvere et al., 2019). The term size of functional categories was limited to 10-150 to exclude GO terms associated with general processes, and electronic GO annotations were discarded to increase GO term accuracy.

Statistical analysis

Experiments were performed at least three times. Statistical significance is based on either one- or two-way ANOVA followed by Tukey's post-hoc test performed in the R environment. The multcompView R package (Graves et al., 2019) was used to assign a compact letter display to indicate the statistical differences in post-hoc tests.

Accession numbers

Sequence data from this article can be found in the Solanaceae Genomics Network database (https://solgenomics.net/) under the following accession numbers: *Bsk880* (Solyc01g080880), *Bsk260* (Solyc04g082260), *Bsk600* (Solyc06g076600), *Bsk750* (Solyc09g011750), *Bsk000* (Solyc10g085000), *Bsk890* (Solyc11g064890), *Bsk830* (Solyc12g099830), *Fls2.1* (Solyc02g070890), *Fls2.2* (Solyc02g070910), *Fls3* (Solyc04g009640). RNA-seq reads generated in this work are available under accession number GSE199518 in the NCBI Gene Expression Omnibus (GEO) database.

AKNOWLEDGMENTS

We thank Mary Beth Mudgett for providing the *Pst* DC3118 strain and Doron Teper for critical reading of the manuscript. This work was supported by grants from the United States-Israel Binational Agricultural Research and Development Fund (BARD; grant no. IS-4931-16C and IS-3541-21C to G.S. and G.B.M.) and the National Science Foundation (grant no. IOS-1546625 to G.B.M).

AUTHOR CONTRIBUTIONS

G.So., B.B.M., G.B.M., and G.S. conceived and designed the experimental plans and analyzed the data; B.B.M. performed the protein-protein interaction analyses, and G.So. performed all the other experiments; N.Z. and H.M.R. generated the *bsk830* mutant plants; M.P.C. analyzed the RNA-seq data; G.So. and G.S. wrote the article.

REFERENCES

Andolfo G, Sanseverino W, Rombauts S, Peer Y, Bradeen JM, Carputo D, Frusciante L, Ercolano MR (2013) Overview of tomato (*Solanum lycopersicum*) candidate pathogen recognition genes reveals important *Solanum R* locus dynamics. New Phytol **197**: 223–237

Arnaud D, Hwang I (2015) A sophisticated network of signaling pathways regulates stomatal defenses to bacterial pathogens. Mol Plant **8**: 566–581

Attaran E, Major IT, Cruz JA, Rosa BA, Koo AJK, Chen J, Kramer DM, He SY, Howe GA (2014) Temporal dynamics of growth and photosynthesis suppression in response to jasmonate signaling. Plant Physiol **165**: 1302–1314

Chen H, Zou Y, Shang Y, Lin H, Wang Y, Cai R, Tang X, Zhou J-M (2008) Firefly luciferase complementation imaging assay for protein-protein interactions in plants. Plant Physiol **146**: 368–376

Clarke CR, Chinchilla D, Hind SR, Taguchi F, Miki R, Ichinose Y, Martin GB, Leman S, Felix G, Vinatzer BA (2013) Allelic variation in two distinct *Pseudomonas syringae* flagellin epitopes modulates the strength of plant immune responses but not bacterial motility. New Phytol **200**: 847–860

Deblaere R, Bytebier B, De Greve H, Deboeck F, Schell J, Van Montagu M, Leemans J (1985) Efficient octopine Ti plasmid-derived vectors for *Agrobacterium*-mediated gene transfer to plants. Nucleic Acids Res **13**: 4777–4788

DeFalco TA, Zipfel C (2021) Molecular mechanisms of early plant pattern-triggered immune signaling. Mol Cell **81**: 3449–3467

680 **Dobin A, Davis CA, Schlesinger F, Drenkow J, Zaleski C, Jha S, Batut P,**
681 **Chaisson M, Gingeras TR** (2013) STAR: ultrafast universal RNA-seq aligner.
682 Bioinformatics **29**: 15–21

683 **Du M, Zhai Q, Deng L, Li S, Li H, Yan L, Huang Z, Wang B, Jiang H, Huang T, et**
684 **al** (2014) Closely related NAC transcription factors of tomato differentially
685 regulate stomatal closure and reopening during pathogen attack. Plant Cell **26**:
686 3167–3184

687 **Du M, Zhao J, Tzeng DTW, Liu Y, Deng L, Yang T, Zhai Q, Wu F, Huang Z, Zhou**
688 **M, et al** (2017) MYC2 orchestrates a hierarchical transcriptional cascade that
689 regulates jasmonate-mediated plant immunity in tomato. Plant Cell **29**: 1883–
690 1906

691 **Duxbury Z, Wu C, Ding P** (2021) A comparative overview of the intracellular
692 guardians of plants and animals: NLRs in innate immunity and beyond. Annu
693 Rev Plant Biol **72**: 155–184

694 **Frary A, Van Eck J** (2005) Organogenesis from transformed tomato explants.
695 Transgenic plants: methods and protocols pp. 141–150

696 **Frederick RD, Thilmony RL, Sessa G, Martin GB** (1998) Recognition specificity for
697 the bacterial avirulence protein AvrPto is determined by Thr-204 in the activation
698 loop of the tomato Pto kinase. Mol Cell **2**: 241–245

699 **Gimenez-Ibanez S, Boter M, Fernández-Barbero G, Chini A, Rathjen JP, Solano**
700 **R** (2014) The bacterial effector HopX1 targets JAZ transcriptional repressors to
701 activate jasmonate signaling and promote infection in *Arabidopsis*. PLoS Biol
702 **12**: e1001792

703 **Gimenez-Ibanez S, Boter M, Ortigosa A, García-Casado G, Chini A, Lewsey MG,**
704 **Ecker JR, Ntoukakis V, Solano R** (2017) JAZ2 controls stomata dynamics
705 during bacterial invasion. New Phytol **213**: 1378–1392

706 **Gómez-Gómez L, Boller T** (2000) FLS2: an LRR receptor-like kinase involved in the
707 perception of the bacterial elicitor flagellin in Arabidopsis. Mol Cell **5**: 1003–11

708 **Goodin MM, Zaitlin D, Naidu RA, Lommel SA** (2008) *Nicotiana benthamiana*: its
709 history and future as a model for plant-pathogen interactions. Mol Plant Microbe
710 Interact **21**: 1015–1026

711 **Graves S, Piepho HP, Selzer L** (2019) multcompView: Visualizations of paired
712 comparisons. R package version 0.1-8. Available at: https://cran.r-
713 project.org/package=multcompView.

714 **Guo H, Nolan TM, Song G, Liu S, Xie Z, Chen J, Schnable PS, Walley JW, Yin Y**
715 (2018) FERONIA receptor kinase contributes to plant immunity by suppressing
716 jasmonic acid signaling in *Arabidopsis thaliana*. Curr Biol **28**: 3316-3324.e6

717 **Guo M, Tian F, Wamboldt Y, Alfano JR** (2009) The majority of the type III effector
718 inventory of *Pseudomonas syringae* pv. *tomato* DC3000 can suppress plant
719 immunity. Mol Plant-Microbe Interact **22**: 1069–1080

720 **Guzel Deger A, Scherzer S, Nuhkat M, Kedzierska J, Kollist H, Brosché M,**
721 **Unyayar S, Boudsocq M, Hedrich R, Roelfsema MRG** (2015) Guard cell
722 SLAC1-type anion channels mediate flagellin-induced stomatal closure. New
723 Phytol **208**: 162–173

724 **Guzman AR, Kim J-G, Taylor KW, Lanver D, Mudgett MB** (2020) Tomato Atypical
725 Receptor Kinase1 is involved in the regulation of preinvasion defense. Plant

726 Physiol **183**: 1306–1318

727 **Hind SR, Strickler SR, Boyle PC, Dunham DM, Bao Z, O'Doherty IM, Baccile JA,**
728 **Hoki JS, Viox EG, Clarke CR, et al** (2016a) Tomato receptor FLAGELLIN-
729 SENSING 3 binds flgII-28 and activates the plant immune system. Nat Plants **2**:
730 1–8

731 **Jacobs TB, LaFayette PR, Schmitz RJ, Parrott WA** (2015) Targeted genome
732 modifications in soybean with CRISPR/Cas9. BMC Biotechnol **15**: 16

733 **Jacobs TB, Zhang N, Patel D, Martin GB** (2017) Generation of a collection of
734 mutant tomato lines using pooled CRISPR libraries. Plant Physiol **174**: 2023–
735 2037

736 **Jarad M, Mariappan K, Almeida-Trapp M, Mette MF, Mithöfer A, Rayapuram N,**
737 **Hirt H** (2020) The Lamin-Like LITTLE NUCLEI 1 (LINC1) regulates pattern-
738 triggered immunity and jasmonic acid signaling. Front Plant Sci. 1639

739 **Jia Z, Giehl RFH, Meyer RC, Altmann T, von Wirén N** (2019) Natural variation of
740 BSK3 tunes brassinosteroid signaling to regulate root foraging under low
741 nitrogen. Nat Commun **10**: 2378

742 **Jiang S, Yao J, Ma K-W, Zhou H, Song J, He SY, Ma W** (2013) Bacterial effector
743 activates jasmonate signaling by directly targeting JAZ transcriptional
744 repressors. PLoS Pathog **9**: e1003715

745 **Kadota Y, Sklenar J, Derbyshire P, Stransfeld L, Asai S, Ntoukakis V, Jones JD,**
746 **Shirasu K, Menke F, Jones A, et al** (2014a) Direct regulation of the NADPH
747 oxidase RBOHD by the PRR-associated kinase BIK1 during plant immunity. Mol
748 Cell **54**: 43–55

749 **Katsir L, Schilmiller AL, Staswick PE, He SY, Howe GA** (2008) COI1 is a critical
750 component of a receptor for jasmonate and the bacterial virulence factor
751 coronatine. Proc Natl Acad Sci **105**: 7100–7105

752 **Krol E, Mentzel T, Chinchilla D, Boller T, Felix G, Kemmerling B, Postel S,**
753 **Arents M, Jeworutzki E, Al-Rasheid KAS, et al** (2010) Perception of the
754 *Arabidopsis* danger signal peptide 1 involves the pattern recognition receptor
755 *At*PEPR1 and its close homologue *At*PEPR2. J Biol Chem **285**: 13471–13479

756 **Kvitko BH, Park DH, Velásquez AC, Wei C-F, Russell AB, Martin GB, Schneider**
757 **DJ, Collmer A** (2009) Deletions in the repertoire of *Pseudomonas syringae* pv.
758 *tomato* DC3000 type III secretion effector genes reveal functional overlap
759 among effectors. PLoS Pathog **5**: e1000388

760 **Larsson J** (2020) eulerr: Area-proportional euler and venn diagrams with ellipses. R
761 package version 6.1.0. Available at: https://cran.r-project.org/package=eulerr.

762 **Lee S, Ishiga Y, Clermont K, Mysore KS** (2013) Coronatine inhibits stomatal
763 closure and delays hypersensitive response cell death induced by nonhost
764 bacterial pathogens. PeerJ **1**: e34

765 **Li L, Li M, Yu L, Zhou Z, Liang X, Liu Z, Cai G, Gao L, Zhang X, Wang Y, et al.**
766 (2014) The FLS2-associated kinase BIK1 directly phosphorylates the NADPH
767 oxidase RbohD to control plant immunity. Cell Host Microbe **15**: 329–338

768 **Li R, Liu P, Wan Y, Chen T, Wang Q, Mettbach U, Baluška F, Šamaj J, Fang X,**
769 **Lucas WJ, et al.** (2012a) A membrane microdomain-associated protein,
770 *Arabidopsis* Flot1, is involved in a clathrin-independent endocytic pathway and
771 is required for seedling development. Plant Cell **24**: 2105–2122

772 **Li ZY, Xu ZS, He GY, Yang GX, Chen M, Li LC, Ma YZ** (2012b) A mutation in
773 *Arabidopsis BSK5* encoding a brassinosteroid-signaling kinase protein affects
774 responses to salinity and abscisic acid. Biochem Biophys Res Commun **426**:
775 522–527

776 **Liang X, Zhou J-M** (2018) Receptor-like cytoplasmic kinases: Central players in
777 plant receptor kinase–mediated signaling. Annu Rev Plant Biol **69**: 267–299

778 **Liu Y, Maierhofer T, Rybak K, Sklenar J, Breakspear A, Johnston MG,**
779 **Fliegmann J, Huang S, Roelfsema MRG, Felix G, et al** (2019) Anion channel
780 SLAH3 is a regulatory target of chitin receptor-associated kinase PBL27 in
781 microbial stomatal closure. Elife. **8**: e44474

782 **Ma L, Salas O, Bowler K, Oren-Young L, Bar-Peled M, Sharon A** (2017) Genetic
783 alteration of UDP-rhamnose metabolism in *Botrytis cinerea* leads to the
784 accumulation of UDP-KDG that adversely affects development and
785 pathogenicity. Mol Plant Pathol **18**: 263–275

786 **Ma SW, Morris, VL, Cuppels DA** (1991) Characterization of a DNA region required
787 for production of the phytotoxin coronatine by *Pseudomonas syringae* pv.
788 *tomato*. Mol Plant-Microbe Interact **4**: 69

789 **Majhi BB, Sobol G, Gachie S, Sreeramulu S, Sessa G** (2021)
790 BRASSINOSTEROID-SIGNALLING KINASES 7 and 8 associate with the FLS2
791 immune receptor and are required for flg22-induced PTI responses. Mol Plant
792 Pathol **22**: 786–799

793 **Majhi BB, Sreeramulu S, Sessa G** (2019) BRASSINOSTEROID-SIGNALING
794 KINASE5 associates with immune receptors and is required for immune
795 responses. Plant Physiol **180**: 1166–1184

796 **Melotto M, Underwood W, Koczan J, Nomura K, He SY** (2006) Plant stomata
797 function in innate immunity against bacterial invasion. Cell **126**: 969–980

798 **Melotto M, Zhang L, Oblessuc PR, He SY** (2017) Stomatal defense a decade later.
799 Plant Physiol **174**: 561–571

800 **Mortazavi A, Williams BA, McCue K, Schaeffer L, Wold B** (2008) Mapping and
801 quantifying mammalian transcriptomes by RNA-Seq. Nat Methods **5**: 621–628

802 **Murray MG, Thompson WF** (1980) Rapid isolation of high molecular weight plant
803 DNA. Nucleic Acids Res **8**: 4321–4326

804 **Ooms G, Hooykaas PJJ, Van Veen RJM, Van Beelen P, Regensburg-Tuïnk TJG,**
805 **Schilperoort RA** (1982) Octopine Ti-plasmid deletion mutants of *Agrobacterium*
806 *tumefaciens* with emphasis on the right side of the T-region. Plasmid **7**: 15–29

807 **Popov G, Fraiture M, Brunner F, Sessa G** (2016) Multiple *Xanthomonas*
808 *euvesicatoria* type III effectors inhibit flg22-triggered immunity. Mol Plant
809 Microbe Interact **29**: 651–660

810 **Rao S, Zhou Z, Miao P, Bi G, Hu M, Wu Y, Feng F, Zhang X, Zhou J-M** (2018)
811 Roles of receptor-like cytoplasmic kinase VII members in pattern-triggered
812 immune signaling. Plant Physiol **177**: 1679-1690

813 **Raudvere U, Kolberg L, Kuzmin I, Arak T, Adler P, Peterson H, Vilo J** (2019)
814 g:Profiler: a web server for functional enrichment analysis and conversions of
815 gene lists (2019 update). Nucleic Acids Res **47**: W191–W198

816 **Ren H, Willige BC, Jaillais Y, Geng S, Park MY, Gray WM, Chory J** (2019)
817 BRASSINOSTEROID-SIGNALING KINASE 3, a plasma membrane-associated
818 scaffold protein involved in early brassinosteroid signaling. PLOS Genet **15**:

819 e1007904

820 **Robatzek S, Bittel P, Chinchilla D, Köchner P, Felix G, Shiu S-H, Boller T** (2007)
821 Molecular identification and characterization of the tomato flagellin receptor
822 LeFLS2, an orthologue of *Arabidopsis* FLS2 exhibiting characteristically different
823 perception specificities. Plant Mol Biol **64**: 539–47

824 **Roberts R, Hind SR, Pedley KF, Diner BA, Szarzanowicz MJ, Luciano-Rosario**
825 **D, Majhi BB, Popov G, Sessa G, Oh C-S, et al.** (2019a) Mai1 protein acts
826 between host recognition of pathogen effectors and mitogen-activated protein
827 kinase signaling. Mol Plant-Microbe Interact **32**: 1496–1507

828 **Roberts R, Mainiero S, Powell AF, Liu AE, Shi K, Hind SR, Strickler SR, Collmer**
829 **A, Martin GB** (2019b) Natural variation for unusual host responses and flagellin-
830 mediated immunity against *Pseudomonas syringae* in genetically diverse tomato
831 accessions. New Phytol **223**: 447–461

832 **Roberts R, Liu AE, Wan L, Geiger AM, Hind SR, Rosli HG, Martin GB** (2020)
833 Molecular characterization of differences between the tomato immune receptors
834 Flagellin sensing 3 and Flagellin sensing 2. Plant Physiol **183**: 1825–1837

835 **Rosli HG, Zheng Y, Pombo MA, Zhong S, Bombarely A, Fei Z, Collmer A, Martin**
836 **GB** (2013) Transcriptomics-based screen for genes induced by flagellin and
837 repressed by pathogen effectors identifies a cell wall-associated kinase involved
838 in plant immunity. Genome Biol **14**: 1-15

839 **Salomon D, Sessa G** (2010) Identification of growth inhibition phenotypes induced
840 by expression of bacterial type III effectors in yeast. J Vis Exp. **37**: e1865

841 **Sasaki-Sekimoto Y, Jikumaru Y, Obayashi T, Saito H, Masuda S, Kamiya Y,**

Ohta H, Shirasu K (2013) Basic helix-loop-helix transcription factors JASMONATE-ASSOCIATED MYC2-LIKE1 (JAM1), JAM2, and JAM3 are negative regulators of jasmonate responses in arabidopsis. Plant Physiol **163**: 291–304

Shi H, Li Q, Luo M, Yan H, Xie B, Li X, Zhong G, Chen D, Tang D (2022) BRASSINOSTEROID-SIGNALING KINASE1 modulates MAP KINASE15 phosphorylation to confer powdery mildew resistance in *Arabidopsis*. Plant Cell.

Shi H, Shen Q, Qi Y, Yan H, Nie H, Chen Y, Zhao T, Katagiri F, Tang D (2013) BR-SIGNALING KINASE1 physically associates with FLAGELLIN SENSING2 and regulates plant innate immunity in *Arabidopsis*. Plant Cell **25**: 1143–1157

Sierla M, Waszczak C, Vahisalu T, Kangasjärvi J (2016) Reactive oxygen species in the regulation of stomatal movements. Plant Physiol **171**: 1569–1580

Singh DK, Calviño M, Brauer EK, Fernandez-Pozo N, Strickler S, Yalamanchili R, Suzuki H, Aoki K, Shibata D, Stratmann JW, et al. (2014) The tomato kinome and the tomato kinase library ORFeome: Novel resources for the study of kinases and signal transduction in tomato and *Solanaceae* species. Mol Plant-Microbe Interact **27**: 7–17

Smirnova E, Marquis V, Poirier L, Aubert Y, Zumsteg J, Ménard R, Miesch L, Heitz T (2017) Jasmonic Acid Oxidase 2 hydroxylates jasmonic acid and represses basal defense and resistance responses against *Botrytis cinerea* infection. Mol Plant **10**: 1159–1173

Sreeramulu S, Mostizky Y, Sunitha S, Shani E, Nahum H, Salomon D, Hayun L Ben, Gruetter C, Rauh D, Ori N, et al. (2013) BSKs are partially redundant positive regulators of brassinosteroid signaling in *Arabidopsis*. Plant J **74**: 905–

919

Su B, Wang A, Shan X (2022) The role of *N*-myristoylation in homeostasis of brassinosteroid signaling kinase 1. Planta **255**: 73

Su B, Zhang X, Li L, Abbas S, Yu M, Cui Y, Baluška F, Hwang I, Shan X, Lin J (2021) Dynamic spatial reorganization of BSK1 complexes in the plasma membrane underpins signal-specific activation for growth and immunity. Mol Plant **14**: 588–603

Tang W, Kim T-W, Oses-Prieto JA, Sun Y, Deng Z, Zhu S, Wang R, Burlingame AL, Wang Z-Y (2008) BSKs mediate signal transduction from the receptor kinase BRI1 in *Arabidopsis*. Science **321**: 557–60

Thaler JS, Humphrey PT, Whiteman NK (2012) Evolution of jasmonate and salicylate signal crosstalk. Trends Plant Sci **17**: 260–270

Thor K, Jiang S, Michard E, George J, Scherzer S, Huang S, Dindas J, Derbyshire P, Leitão N, DeFalco TA, et al (2020) The calcium-permeable channel OSCA1.3 regulates plant stomatal immunity. Nature **585**: 569–573

Tian W, Hou C, Ren Z, Wang C, Zhao F, Dahlbeck D, Hu S, Zhang L, Niu Q, Li L, et al (2019) A calmodulin-gated calcium channel links pathogen patterns to plant immunity. Nature **572**: 131–135

Tomato Genome Consortium (2012) The tomato genome sequence provides insights into fleshy fruit evolution. Nature **485**: 635–641

Toum L, Torres PS, Gallego SM, Benavídes MP, Vojnov AA, Gudesblat GE (2016) Coronatine inhibits stomatal closure through guard cell-specific inhibition of NADPH oxidase-dependent ROS production. Front Plant Sci. 1851

889 **Vanholme R, De Meester B, Ralph J, Boerjan W** (2019) Lignin biosynthesis and its
890 integration into metabolism. Curr Opin Biotechnol **56**: 230-239.

891 **Wang H, Hutton SF, Robbins MD, Sim S-C, Scott JW, Yang W, Jones JB,**
892 **Francis DM** (2011) Molecular mapping of hypersensitive resistance from tomato
893 'Hawaii 7981' to *Xanthomonas perforans* race T3. Phytopathology **101**: 1217–
894 1223

895 **Wang L, Albert M, Einig E, Fürst U, Krust D, Felix G** (2016) The pattern-
896 recognition receptor CORE of Solanaceae detects bacterial cold-shock protein.
897 Nat Plants **2**: 16185

898 **Wang Z, Gou X** (2021) The first line of defense: Receptor-like protein kinase-
899 mediated stomatal immunity. Int J Mol Sci **23**: 343

900 **Wasternack C, Song S** (2016) Jasmonates: biosynthesis, metabolism, and signaling
901 by proteins activating and repressing transciption. J Exp Bot **68**: 1303-1321

902 **Weyers JDB, Johansen LG** (1985) Accurate estimation of stomatal aperture from
903 silicone rubber impressions. New Phytol **101**: 109–115

904 **Wilson M, Campbell HL, Ji P, Jones JB, Cuppels DA** (2002) Biological control of
905 bacterial speck of tomato under field conditions at several locations in north
906 america. Phytopathology **92**: 1284–1292

907 **Xing Y** (2006) An expectation-maximization algorithm for probabilistic
908 reconstructions of full-length isoforms from splice graphs. Nucleic Acids Res **34**:
909 3150–3160

910 **Xu P, Xu S-L, Li Z-J, Tang W, Burlingame AL, Wang Z-Y** (2014) A
911 brassinosteroid-signaling kinase interacts with multiple receptor-like kinases in

912 *Arabidopsis*. Mol Plant **7**: 441–444

913 **Yan H, Zhao Y, Shi H, Li J, Wang Y, Tang D** (2018) BRASSINOSTEROID-
914 SIGNALING KINASE1 phosphorylates MAPKKK5 to regulate immunity in
915 *Arabidopsis*. Plant Physiol **176**: 2991-3002

916 **Yi SY, Shirasu K, Moon JS, Lee S-G, Kwon S-Y** (2014) The activated SA and JA
917 signaling pathways have an influence on flg22-triggered oxidative burst and
918 callose deposition. PLoS One **9**: e88951

919 **Zhang L, Zhang F, Melotto M, Yao J, He SY** (2017) Jasmonate signaling and
920 manipulation by pathogens and insects. J Exp Bot **68**: 1371-1385

921 **Zhang N, Pombo MA, Rosli HG, Martin GB** (2020) Tomato wall-associated kinase
922 SlWak1 depends on Fls2/Fls3 to promote apoplastic immune responses to
923 *Pseudomonas syringae*. Plant Physiol **183**: 1869–1882

924 **Zheng X, Kang S, Jing Y, Ren Z, Li L, Zhou J-M, Berkowitz G, Shi J, Fu A, Lan W,**
925 **et al** (2018) Danger-associated peptides close stomata by OST1-independent
926 activation of anion channels in guard cells. Plant Cell **30**: 1132–1146

927 **Zheng X, Spivey NW, Zeng W, Liu P-P, Fu ZQ, Klessig DF, He SY, Dong X**
928 (2012) Coronatine promotes *Pseudomonas syringae* virulence in plants by
929 activating a signaling cascade that inhibits salicylic acid accumulation. Cell Host
930 Microbe **11**: 587–596

931 **Zipfel C, Robatzek S, Navarro L, Oakeley EJ, Jones JDG, Felix G, Boller T**
932 (2004) Bacterial disease resistance in *Arabidopsis* through flagellin perception.
933 Nature **428**: 764–767

934

935 **Table 1.** Functional categories overrepresented in DEGs of *Pf* treated *bsk830* plants.

Up-regulated genes		
Term name	**Term ID**	**$-\log_{10}(p_{adj})$**
response to chitin	GO:0010200	5.53039
regulation of jasmonic acid mediated signaling pathway	GO:2000022	5.42490
cellular response to fatty acid	GO:0071398	4.02940
jasmonic acid mediated signaling pathway	GO:0009867	3.47824
cellular response to jasmonic acid stimulus	GO:0071395	3.37033
lignin metabolic process	GO:0009808	3.19087
regulation of defense response to insect	GO:2000068	3.18180
phenylpropanoid metabolic process	GO:0009698	2.80966
phenylpropanoid biosynthetic process	GO:0009699	2.19778
regulation of anion channel activity	GO:0010359	2.09635
Down-regulated genes		
Term name	**Term ID**	**$-\log_{10}(p_{adj})$**
photosynthesis, light reaction	GO:0019684	44.88674
photosynthetic electron transport chain	GO:0009767	21.43202
photosynthesis, light harvesting	GO:0009765	17.15130
photosynthesis, light harvesting in photosystem I	GO:0009768	14.07682
electron transport chain	GO:0022900	14.04188
photosynthetic electron transport in photosystem I	GO:0009773	13.60706
NAD(P)H dehydrogenase complex assembly	GO:0010275	11.56992
photosystem II assembly	GO:0010207	7.293742
response to high light intensity	GO:0009644	5.682999
glucose metabolic process	GO:0006006	5.284815

FIGURE LEGENDS

Figure 1. Interaction of Bsk830 with Fls2 and Fls3. A, Yeast cells expressing individual Bsk proteins fused to the GAL4 DNA-binding domain (bait), and the kinase domain of Fls2 ($Fls2_{KD}$) and Fls3 ($Fls3_{KD}$) fused to the GAL4 DNA-activation domain (prey) were grown on synthetically defined medium lacking Leu and Trp (SD–LW), SD–LW lacking His and Ade (SD–LWHA), or SD–LW supplemented with Aureobasidin A (SD–LW+AbA). Empty vectors (EV) were used as negative controls. Nomenclature and accession numbers of tomato Bsk family members are reported in the Materials and Methods section. B, The indicated proteins were fused to C-LUC or N-LUC and co-expressed via *A. tumefaciens* GV2260 in *N. benthamiana* leaves. Luciferase activity was quantified by measuring relative luminescence at 48 h after agro-infiltration. Data from three independent experiments is shown. Circles represent individual data points, and letters represent statistical significance determined by one-way ANOVA and Tukey's post-hoc test ($P < 0.05$).

Figure 2. Bsk830 localizes to the plasma membrane. A, Putative myristoylation and palmitoylation sites at the N-terminus of Bsk830. Bsk830-YFP (B), $Bsk830^{G2A}$-YFP (C), or $Bsk830^{C(3,11,12)A}$-YFP (C) fusion proteins were co-expressed via *A. tumefaciens* GV2260 in *N. benthamiana* leaves with the plasma membrane marker Flot1b-mCherry. Fluorescence was monitored in epidermal cells by confocal microscopy at 48 h after agro-infiltration. YFP, mCherry, and merged fluorescence images are shown. The region marked in the merged image by a dotted square is magnified in the inset panel. Fluorescence intensity was measured in the YFP and mCherry channels along the dotted line. Scale bars represents 20 μm, except for the inset image, where it represents 10 μm.

961

962 **Figure 3.** Bsk830 is required for flagellin-mediated immunity. A, Wild-type and
963 *bsk830* mutant plants were inoculated by dipping into a bacterial suspension
964 (10^7 CFU mL^{-1}) of *Pst* DC3000 or *Pst* DC3000Δ*fliC*. Bacterial populations were
965 measured in leaves at 0 and 2 days post-inoculation (dpi). Circles represent
966 individual data points of three biological replicates, and letters represent statistical
967 significance determined by two-way ANOVA and Tukey's post-hoc test ($P < 0.05$). B
968 and C, ROS production. Leaf discs were treated with 100 nM of flg22, flgII-28, or
969 water. Luminescence was measured for 30 min after flg22 treatment (B) and for 45
970 min after flgII-28 treatment (C). ROS production was normalized to the ROS amount
971 produced by wild-type plants at its peak. Data are means ± SD of three biological
972 replicates.

973

974 **Figure 4.** *bsk830* mutant plants are compromised in stomatal immunity. A and B,
975 Wild-type and *bsk830* mutant plants were inoculated with *Pst* DC3000 by dipping
976 (10^7 CFU mL^{-1}) (A) or vacuum-infiltration (10^5 CFU mL^{-1}) (B). Bacterial populations
977 were measured in leaves at 0 and 2 days post-inoculation (dpi). Data from three
978 independent experiments is shown. C and D, Stomatal aperture index (aperture
979 width divided by the stomata length) was determined in leaves after 0, 1, 2.5, and 4 h
980 floating on suspensions (10^8 CFU mL^{-1}) of *Pst* DC3000 (C) and *Pf* A506 (D), or
981 water (mock). Circles represent mean of three biological replicates. Letters represent
982 statistical significance determined by one-way (A and B) or two-way (C and D)
983 ANOVA and Tukey's post-hoc test ($P < 0.05$).

984

Figure 5. A, Euler diagram representing differentially expressed genes (DEGs) (pFDR < 0.05, fold change > 3, *Pf* vs. mock treatment comparison) in wild-type and *bsk830-1* plants. B, Loss of function in *Bsk830* alters expression of genes involved in JA biosynthesis, catabolism, signaling, and response. Each row represents a single gene accompanied by its Solanaceae Genomics Network accession number. Genes not characterized in tomato are annotated with name of the *Arabidopsis* gene with the highest protein similarity obtained by BLAST. The legend corresponds to relative $\log_2$ fold change values calculated based on a *Pf* vs. mock treatment comparison performed for either wild-type or the *bsk830* mutant line. Grey rectangles represent genes with no fold change value available.

Figure 6. A, Plants of the indicated genotypes were inoculated by dipping with a 10^7 CFU mL^{-1} bacterial suspension of *Pst* DC3000 (COR+) or *Pst* DC3118 (COR–). Bacterial populations in leaves were measured at 0 and 2 dpi. B, Plants of the indicated genotypes were vacuum-infiltrated with a *Pf* A506 suspension (10^8 CFU mL^{-1}). After 24 h, plants were inoculated by placing a droplet of a suspension carrying *Botrytis cinerea* spores (2×10^5 conidia mL^{-1}). Lesion area was measured at 3 dpi. In (A and B) data from three independent experiments is shown. Letters represent statistical significance determined by two-way ANOVA and Tukey's post-hoc test ($P < 0.05$).

SUPPLEMENTAL TABLES AND FIGURE LEGENDS

Supplemental Table S1. List of differentially expressed genes.

Supplemental Table S2. Primers used in this study.

Supplemental Figure S1. A, Expression in yeast of the kinase domain of Fls2 ($Fls2_{KD}$) and Fls3 ($Fls3_{KD}$) fused to the GAL4 DNA-activation domain (GAL4-AD). B, Expression in leaves of *N. benthamiana* plants of $Fls2_{KD}$ and $Fls3_{KD}$ fused to the C-terminal half (C-LUC) of the luciferase protein. Proteins were detected by immunoblot analysis using anti-HA antibodies (α-HA) or anti-luciferase antibodies (α-LUC).

Supplemental Figure S2. Bsk830 is not phosphorylated *in vitro* by Fls2 and Fls3. Phosphorylation of the maltose binding protein (MBP)-Bsk830 fusion by the cytoplasmic domain of Fls2 ($Fls2_{CD}$) and Fls3 ($Fls3_{CD}$) fused to MBP was assayed *in vitro* in the presence of [γ-^{32}P]ATP. Proteins were fractionated by SDS-PAGE, blotted onto a PVDF membrane and exposed to autoradiography, or stained with Coomassie Blue.

Supplemental Figure S3. Sequence of the *Bsk830* deletions in the tomato *bsk830-1* and *bsk830-2* mutant lines. Multiple sequence alignment of the *Bsk830* region flanking the gRNA-targeted site in wild-type, *bsk830-1*, and *bsk830-2* plants. In green, the ATG translation start site; in blue, the PAM motif; in pink, the gRNA. A red dotted line represents sequences deleted in the mutant lines.

Supplemental Figure S4. Tomato *bsk830* mutant plants are not impaired in flg22- and flgII-28-induced MAPK activation. Leaf discs of wild-type, *bsk830-1, bsk830-2, fls2.1/fls2.2* and *fls3* mutant plants were floated overnight in water and treated with 1 µM of flg22 (A) or flgII-28 (B). Samples were harvested at 0, 5 and 20 min after treatment and analyzed by immunoblots with anti-pMAPK antibodies (α-pMAPK). Ponceau S staining of RuBisCO is shown as a loading control. Data are representative of three biological repeats.

Supplemental Figure S5. Stomatal number index of wild-type, *bsk830-1,* and *bsk830-2* tomato plants. The number of stomata and epidermal pavement cells was manually counted in a 0.5 mm^2 leaf area and the stomatal number index was calculated as the percentage of stomata per total cells. Approximately 30 images were analyzed for each plant genotype.

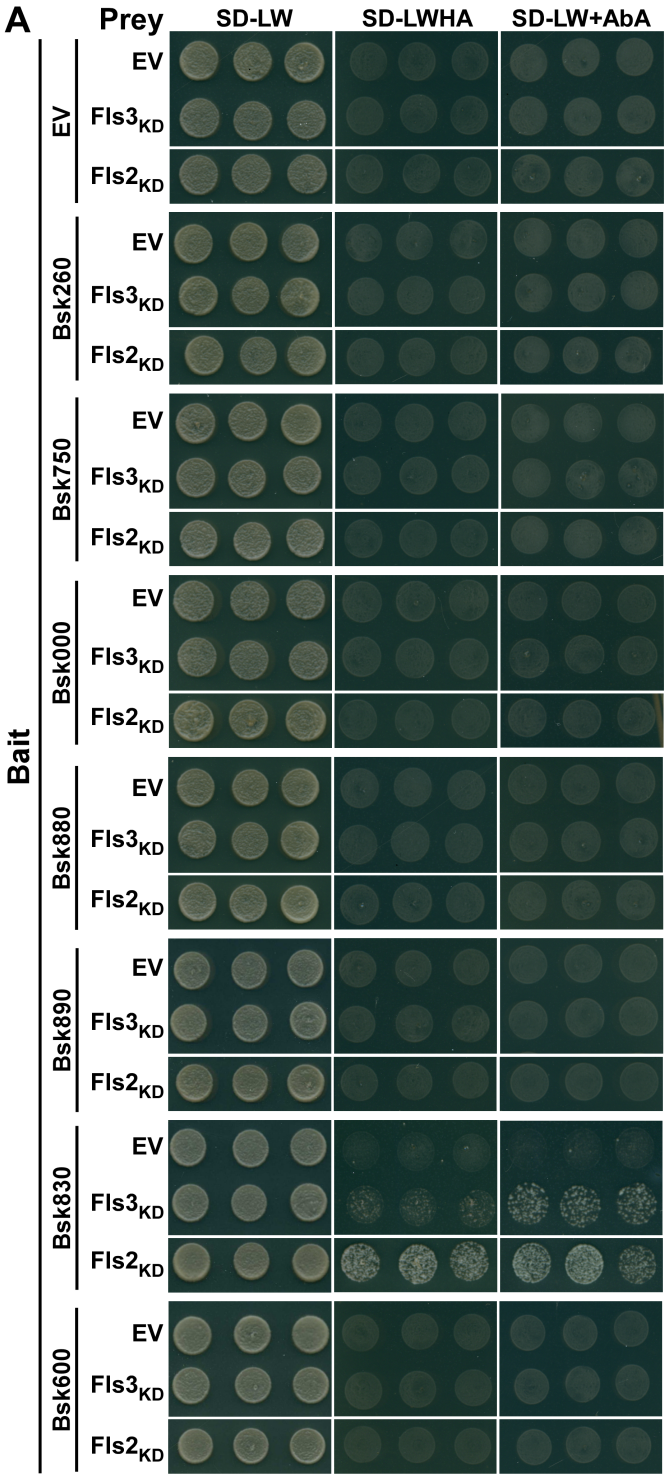

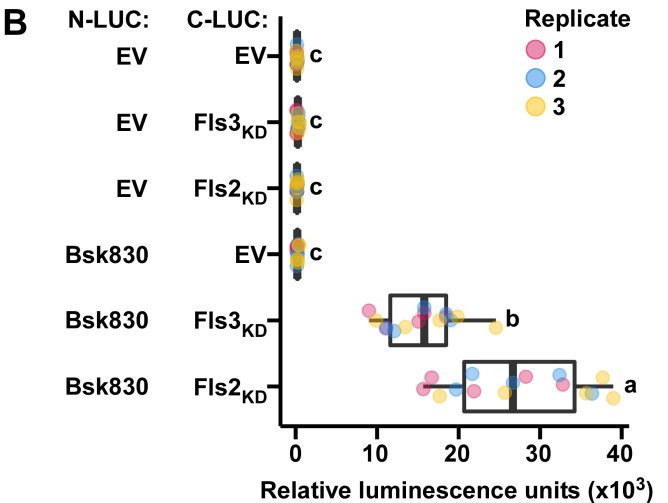

Figure 1. Interaction of Bsk830 with Fls2 and Fls3. A, Yeast cells expressing individual Bsk proteins fused to the GAL4 DNA-binding domain (bait), and the kinase domain of Fls2 ($Fls2_{KD}$) and Fls3 ($Fls3_{KD}$) fused to the GAL4 DNA-activation domain (prey) were grown on synthetically defined medium lacking Leu and Trp (SD–LW), SD–LW lacking His and Ade (SD–LWHA), or SD–LW supplemented with Aureobasidin A (SD–LW+AbA). Empty vectors (EV) were used as negative controls. Nomenclature and accession numbers of tomato Bsk family members are reported in the Materials and Methods section. B, The indicated proteins were fused to C-LUC or N-LUC and co-expressed via *A. tumefaciens* GV2260 in *N. benthamiana* leaves. Luciferase activity was quantified by measuring relative luminescence at 48 h after agro-infiltration. Data from three independent experiments is shown. Circles represent individual data points, and letters represent statistical significance determined by one-way ANOVA and Tukey's post-hoc test ($P < 0.05$).

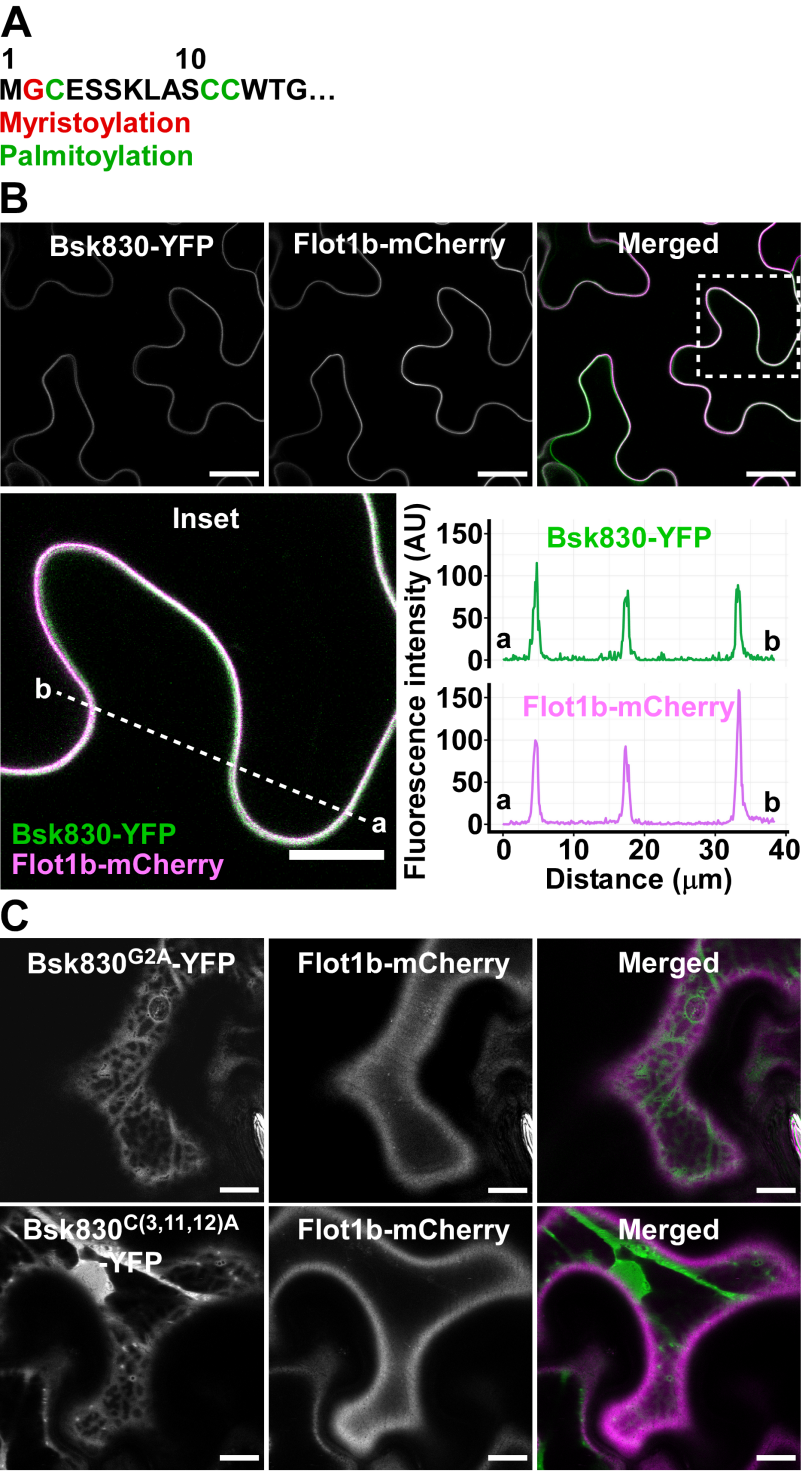

Figure 2. Bsk830 localizes to the plasma membrane. A, Putative myristoylation and palmitoylation sites at the N-terminus of Bsk830. Bsk830-YFP (B), Bsk830^{G2A}-YFP (C), or Bsk830$^{C(3,11,12)A}$-YFP (C) fusion proteins were co-expressed via *A. tumefaciens* GV2260 in *N. benthamiana* leaves with the plasma membrane marker Flot1b-mCherry. Fluorescence was monitored in epidermal cells by confocal microscopy at 48 h after agro-infiltration. YFP, mCherry, and merged fluorescence images are shown. The region marked in the merged image by a dotted square is magnified in the inset panel. Fluorescence intensity was measured in the YFP and mCherry channels along the dotted line. Scale bars represents 20 μm, except for the inset image, where it represents 10 μm.

Sobol et al., Figure 3

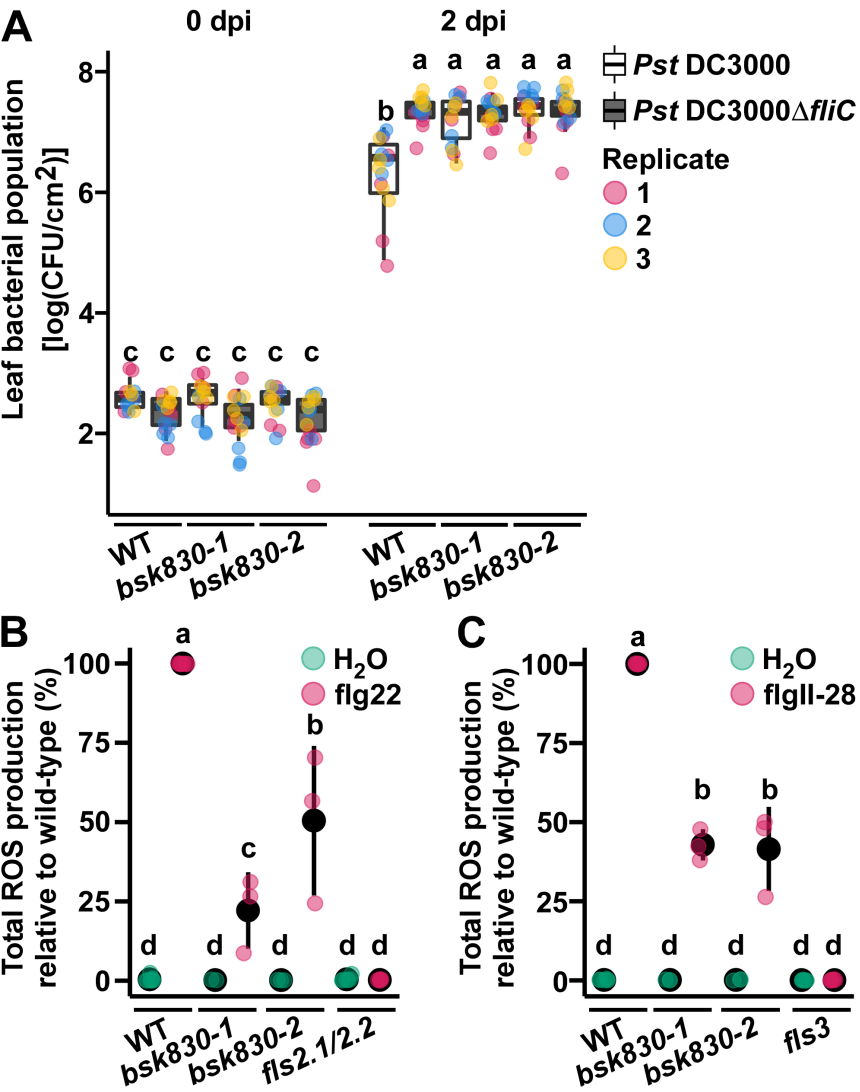

Figure 3. Bsk830 is required for flagellin-mediated immunity. A, Wild-type and *bsk830* mutant plants were inoculated by dipping into a bacterial suspension (10^7 CFU mL^{-1}) of *Pst* DC3000 or *Pst* DC3000Δ*fliC*. Bacterial populations were measured in leaves at 0 and 2 days post-inoculation (dpi). Circles represent individual data points of three biological replicates, and letters represent statistical significance determined by two-way ANOVA and Tukey's post-hoc test ($P < 0.05$). B and C, ROS production. Leaf discs were treated with 100 nM of flg22, flgII-28, or water. Luminescence was measured for 30 min after flg22 treatment (B) and for 45 min after flgII-28 treatment (C). ROS production was normalized to the ROS amount produced by wild-type plants at its peak. Data are means ± SD of three biological replicates.

Sobol et al., Figure 4

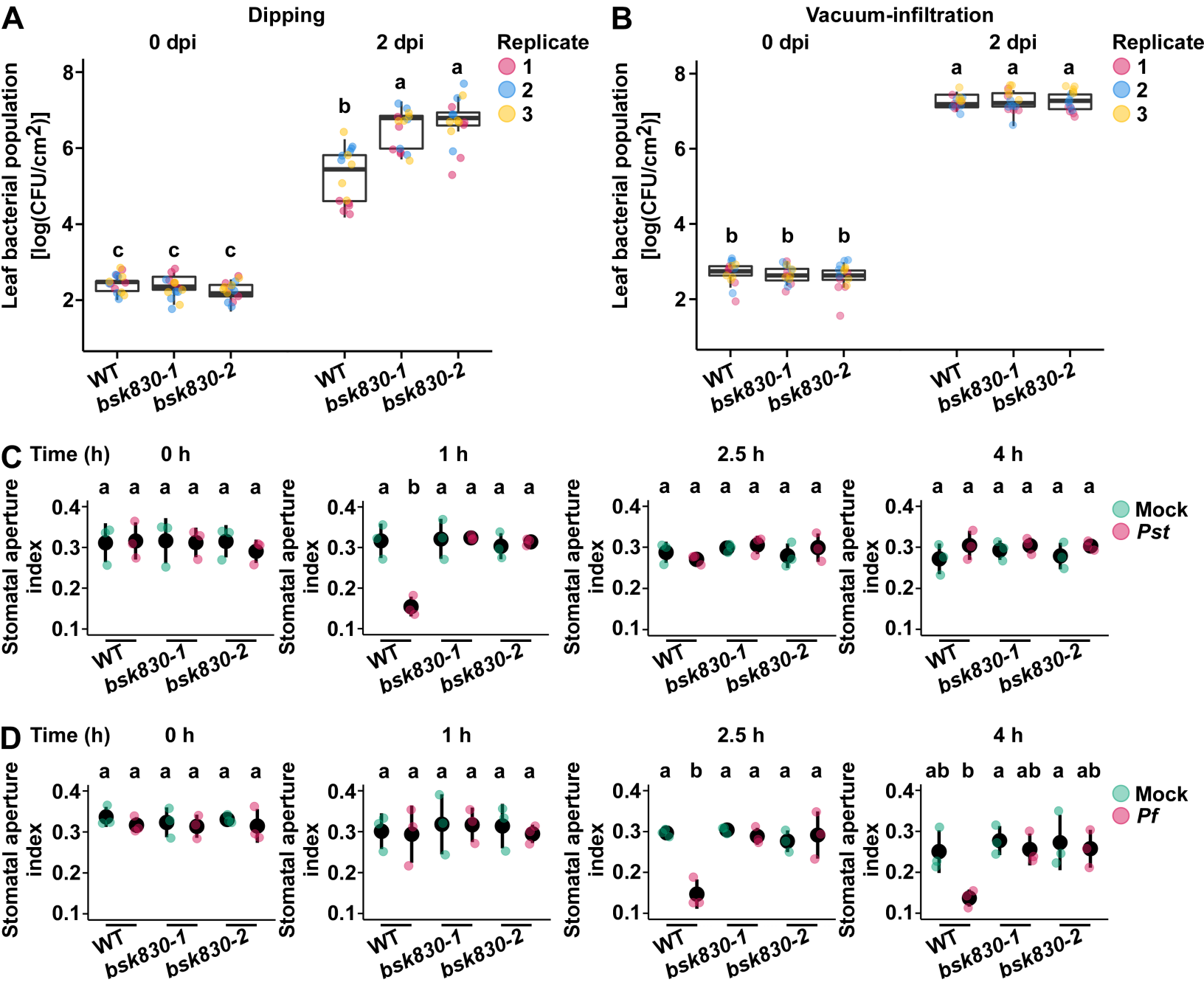

Figure 4. *bsk830* mutant plants are compromised in stomatal immunity. A and B, Wild-type and *bsk830* mutant plants were inoculated with *Pst* DC3000 by dipping (10^7 CFU mL^{-1}) (A) or vacuum-infiltration (10^5 CFU mL^{-1}) (B). Bacterial populations were measured in leaves at 0 and 2 days post-inoculation (dpi). Data from three independent experiments is shown. C and D, Stomatal aperture index (aperture width divided by the stomata length) was determined in leaves after 0, 1, 2.5, and 4 h floating on suspensions (10^8 CFU mL^{-1}) of *Pst* DC3000 (C) and *Pf* A506 (D), or water (mock). Circles represent mean of three biological replicates. Letters represent statistical significance determined by one-way (A and B) or two-way (C and D) ANOVA and Tukey's post-hoc test ($P < 0.05$).

Sobol et al., Figure 5

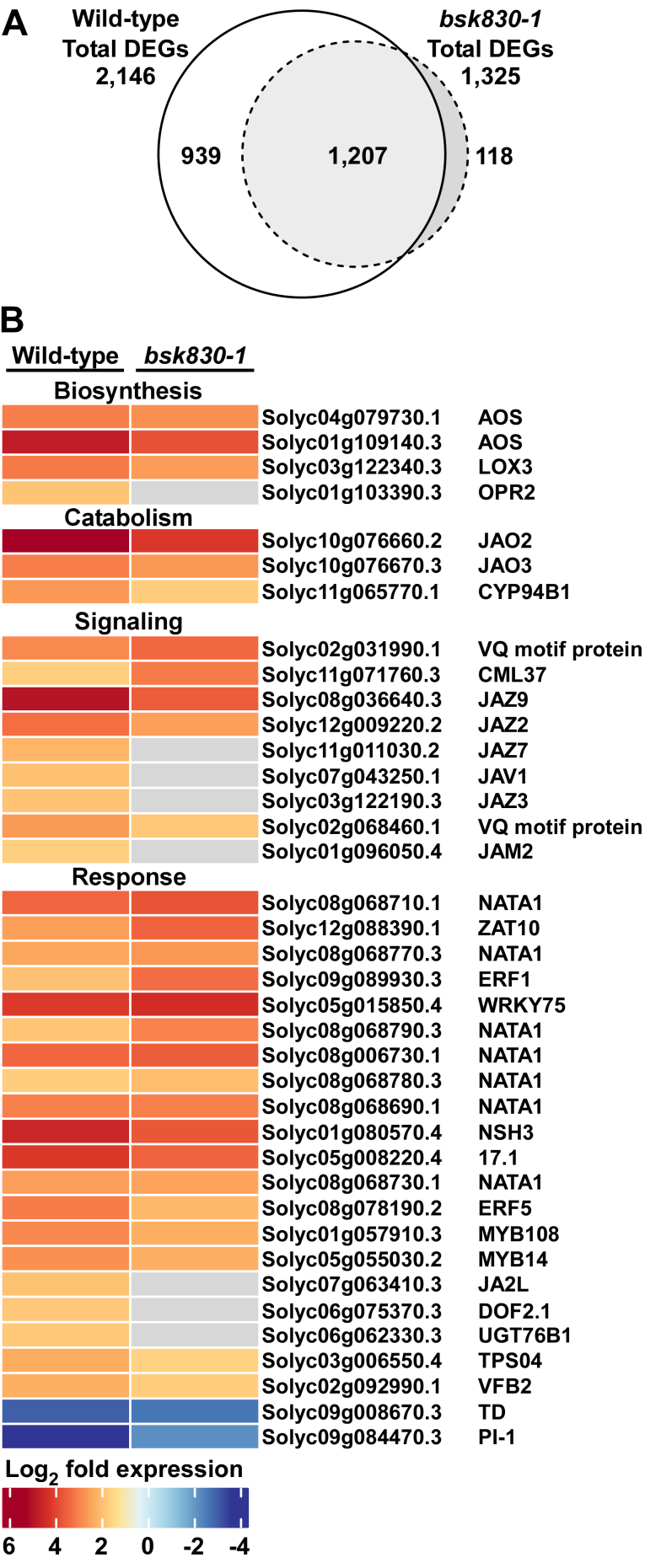

Figure 5. A, Euler diagram representing differentially expressed genes (DEGs) (pFDR < 0.05, fold change > 3, *Pf* vs. mock treatment comparison) in wild-type and *bsk830-1* plants. B, Loss of function in *Bsk830* alters expression of genes involved in JA biosynthesis, catabolism, signaling, and response. Each row represents a single gene accompanied by its Solanaceae Genomics Network accession number. Genes not characterized in tomato are annotated with name of the *Arabidopsis* gene with the highest protein similarity obtained by BLAST. The legend corresponds to relative $\log_2$ fold change values calculated based on a *Pf* vs. mock treatment comparison performed for either wild-type or the *bsk830* mutant line. Grey rectangles represent genes with no fold change value available.

Sobol et al., Figure 6

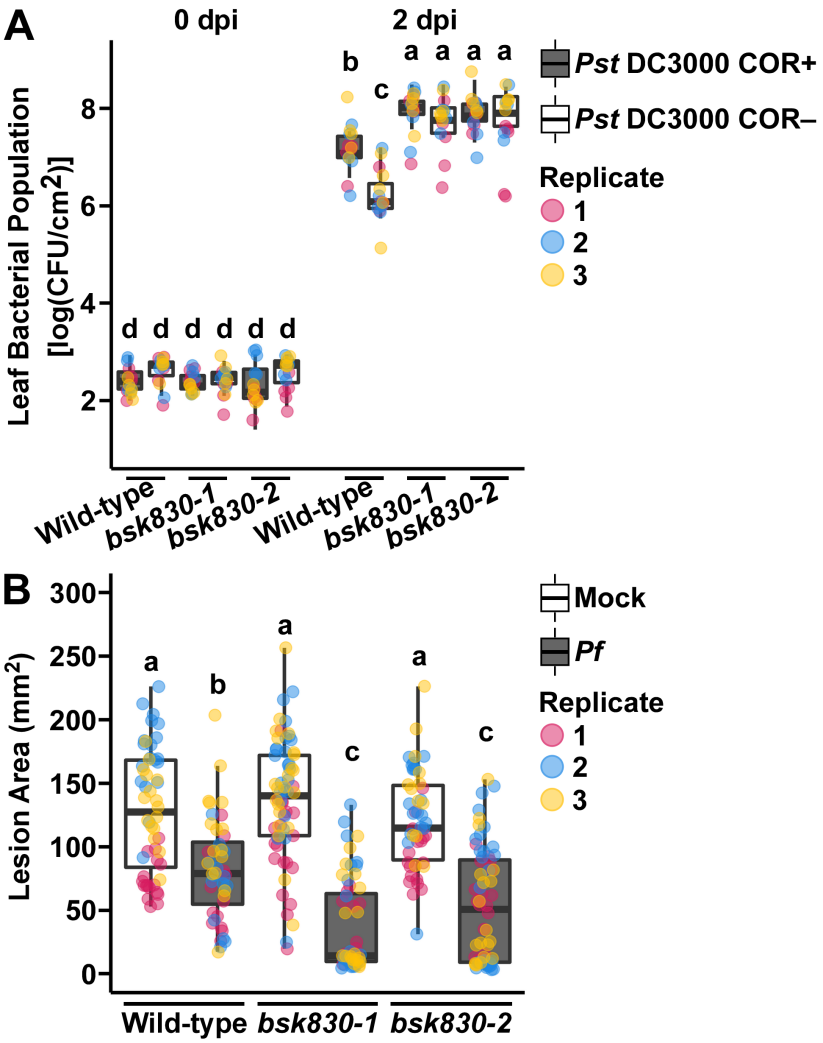

Figure 6. A, Plants of the indicated genotypes were inoculated by dipping with a 10^7 CFU mL^{-1} bacterial suspension of *Pst* DC3000 (COR+) or *Pst* DC3118 (COR–). Bacterial populations in leaves were measured at 0 and 2 dpi. B, Plants of the indicated genotypes were vacuum-infiltrated with a *Pf* A506 suspension (10^8 CFU mL^{-1}). After 24 h, plants were inoculated by placing a droplet of a suspension carrying *Botrytis cinerea* spores (2 x 10^5 conidia mL^{-1}). Lesion area was measured at 3 dpi. In (A and B) data from three independent experiments is shown. Letters represent statistical significance determined by two-way ANOVA and Tukey's post-hoc test ($P < 0.05$).

Parsed Citations

Andolfo G, Sanseverino W, Rombauts S, Peer Y, Bradeen JM, Carputo D, Frusciante L, Ercolano MR (2013) Overview of tomato (Solanum lycopersicum) candidate pathogen recognition genes reveals important Solanum R locus dynamics. New Phytol 197: 223–237
Google Scholar: Author Only Title Only Author and Title

Arnaud D, Hwang I (2015) A sophisticated network of signaling pathways regulates stomatal defenses to bacterial pathogens. Mol Plant 8: 566–581
Google Scholar: Author Only Title Only Author and Title

Attaran E, Major IT, Cruz JA, Rosa BA, Koo AJK, Chen J, Kramer DM, He SY, Howe GA (2014) Temporal dynamics of growth and photosynthesis suppression in response to jasmonate signaling. Plant Physiol 165: 1302–1314
Google Scholar: Author Only Title Only Author and Title

Chen H, Zou Y, Shang Y, Lin H, Wang Y, Cai R, Tang X, Zhou J-M (2008) Firefly luciferase complementation imaging assay for protein-protein interactions in plants. Plant Physiol 146: 368–376
Google Scholar: Author Only Title Only Author and Title

Clarke CR, Chinchilla D, Hind SR, Taguchi F, Miki R, Ichinose Y, Martin GB, Leman S, Felix G, Vinatzer BA (2013) Allelic variation in two distinct Pseudomonas syringae flagellin epitopes modulates the strength of plant immune responses but not bacterial motility. New Phytol 200: 847–860
Google Scholar: Author Only Title Only Author and Title

Deblaere R, Bytebier B, De Greve H, Deboeck F, Schell J, Van Montagu M, Leemans J (1985) Efficient octopine Ti plasmid-derived vectors for Agrobacterium-mediated gene transfer to plants. Nucleic Acids Res 13: 4777–4788
Google Scholar: Author Only Title Only Author and Title

DeFalco TA, Zipfel C (2021) Molecular mechanisms of early plant pattern-triggered immune signaling. Mol Cell 81: 3449–3467
Google Scholar: Author Only Title Only Author and Title

Dobin A, Davis CA, Schlesinger F, Drenkow J, Zaleski C, Jha S, Batut P, Chaisson M, Gingeras TR (2013) STAR: ultrafast universal RNA-seq aligner. Bioinformatics 29: 15–21
Google Scholar: Author Only Title Only Author and Title

Du M, Zhai Q, Deng L, Li S, Li H, Yan L, Huang Z, Wang B, Jiang H, Huang T, et al (2014) Closely related NAC transcription factors of tomato differentially regulate stomatal closure and reopening during pathogen attack. Plant Cell 26: 3167–3184
Google Scholar: Author Only Title Only Author and Title

Du M, Zhao J, Tzeng DTW, Liu Y, Deng L, Yang T, Zhai Q, Wu F, Huang Z, Zhou M, et al (2017) MYC2 orchestrates a hierarchical transcriptional cascade that regulates jasmonate-mediated plant immunity in tomato. Plant Cell 29: 1883–1906
Google Scholar: Author Only Title Only Author and Title

Duxbury Z, Wu C, Ding P (2021) A comparative overview of the intracellular guardians of plants and animals: NLRs in innate immunity and beyond. Annu Rev Plant Biol 72: 155–184
Google Scholar: Author Only Title Only Author and Title

Frary A, Van Eck J (2005) Organogenesis from transformed tomato explants. Transgenic plants: methods and protocols pp. 141–150
Google Scholar: Author Only Title Only Author and Title

Frederick RD, Thilmony RL, Sessa G, Martin GB (1998) Recognition specificity for the bacterial avirulence protein AvrPto is determined by Thr-204 in the activation loop of the tomato Pto kinase. Mol Cell 2: 241–245
Google Scholar: Author Only Title Only Author and Title

Gimenez-Ibanez S, Boter M, Fernández-Barbero G, Chini A, Rathjen JP, Solano R (2014) The bacterial effector HopX1 targets JAZ transcriptional repressors to activate jasmonate signaling and promote infection in Arabidopsis. PLoS Biol 12: e1001792
Google Scholar: Author Only Title Only Author and Title

Gimenez-Ibanez S, Boter M, Ortigosa A, García-Casado G, Chini A, Lewsey MG, Ecker JR, Ntoukakis V, Solano R (2017) JAZ2 controls stomata dynamics during bacterial invasion. New Phytol 213: 1378–1392
Google Scholar: Author Only Title Only Author and Title

Gómez-Gómez L, Boller T (2000) FLS2: an LRR receptor-like kinase involved in the perception of the bacterial elicitor flagellin in Arabidopsis. Mol Cell 5: 1003–11
Google Scholar: Author Only Title Only Author and Title

Goodin MM, Zaitlin D, Naidu RA, Lommel SA (2008) Nicotiana benthamiana: its history and future as a model for plant-pathogen interactions. Mol Plant Microbe Interact 21: 1015–1026
Google Scholar: Author Only Title Only Author and Title

Graves S, Piepho HP, Selzer L (2019) multcompView: Visualizations of paired comparisons. R package version 0.1-8. Available at: https://cran.r-project.org/package=multcompView.
Google Scholar: Author Only Title Only Author and Title

Guo H, Nolan TM, Song G, Liu S, Xie Z, Chen J, Schnable PS, Walley JW, Yin Y (2018) FERONIA receptor kinase contributes to plant immunity by suppressing jasmonic acid signaling in Arabidopsis thaliana. Curr Biol 28: 3316-3324.e6
Google Scholar: Author Only Title Only Author and Title

Guo M, Tian F, Wamboldt Y, Alfano JR (2009) The majority of the type III effector inventory of Pseudomonas syringae pv. tomato DC3000 can suppress plant immunity. Mol Plant-Microbe Interact 22: 1069–1080
Google Scholar: Author Only Title Only Author and Title

Guzel Deger A, Scherzer S, Nuhkat M, Kedzierska J, Kollist H, Brosché M, Unyayar S, Boudsocq M, Hedrich R, Roelfsema MRG (2015) Guard cell SLAC1-type anion channels mediate flagellin-induced stomatal closure. New Phytol 208: 162–173
Google Scholar: Author Only Title Only Author and Title

Guzman AR, Kim J-G, Taylor KW, Lanver D, Mudgett MB (2020) Tomato Atypical Receptor Kinase1 is involved in the regulation of preinvasion defense. Plant Physiol 183: 1306–1318
Google Scholar: Author Only Title Only Author and Title

Hind SR, Strickler SR, Boyle PC, Dunham DM, Bao Z, O'Doherty IM, Baccile JA, Hoki JS, Viox EG, Clarke CR, et al (2016a) Tomato receptor FLAGELLIN-SENSING 3 binds flgII-28 and activates the plant immune system. Nat Plants 2: 1–8
Google Scholar: Author Only Title Only Author and Title

Jacobs TB, LaFayette PR, Schmitz RJ, Parrott WA (2015) Targeted genome modifications in soybean with CRISPR/Cas9. BMC Biotechnol 15: 16
Google Scholar: Author Only Title Only Author and Title

Jacobs TB, Zhang N, Patel D, Martin GB (2017) Generation of a collection of mutant tomato lines using pooled CRISPR libraries. Plant Physiol 174: 2023–2037
Google Scholar: Author Only Title Only Author and Title

Jarad M, Mariappan K, Almeida-Trapp M, Mette MF, Mithöfer A, Rayapuram N, Hirt H (2020) The Lamin-Like LITTLE NUCLEI 1 (LINC1) regulates pattern-triggered immunity and jasmonic acid signaling. Front Plant Sci. 1639
Google Scholar: Author Only Title Only Author and Title

Jia Z, Giehl RFH, Meyer RC, Altmann T, von Wirén N (2019) Natural variation of BSK3 tunes brassinosteroid signaling to regulate root foraging under low nitrogen. Nat Commun 10: 2378
Google Scholar: Author Only Title Only Author and Title

Jiang S, Yao J, Ma K-W, Zhou H, Song J, He SY, Ma W (2013) Bacterial effector activates jasmonate signaling by directly targeting JAZ transcriptional repressors. PLoS Pathog 9: e1003715
Google Scholar: Author Only Title Only Author and Title

Kadota Y, Sklenar J, Derbyshire P, Stransfeld L, Asai S, Ntoukakis V, Jones JD, Shirasu K, Menke F, Jones A, et al (2014a) Direct regulation of the NADPH oxidase RBOHD by the PRR-associated kinase BIK1 during plant immunity. Mol Cell 54: 43–55
Google Scholar: Author Only Title Only Author and Title

Katsir L, Schilmiller AL, Staswick PE, He SY, Howe GA (2008) COI1 is a critical component of a receptor for jasmonate and the bacterial virulence factor coronatine. Proc Natl Acad Sci 105: 7100–7105
Google Scholar: Author Only Title Only Author and Title

Krol E, Mentzel T, Chinchilla D, Boller T, Felix G, Kemmerling B, Postel S, Arents M, Jeworutzki E, Al-Rasheid KAS, et al (2010) Perception of the Arabidopsis danger signal peptide 1 involves the pattern recognition receptor AtPEPR1 and its close homologue AtPEPR2. J Biol Chem 285: 13471–13479
Google Scholar: Author Only Title Only Author and Title

Kvitko BH, Park DH, Velásquez AC, Wei C-F, Russell AB, Martin GB, Schneider DJ, Collmer A (2009) Deletions in the repertoire of Pseudomonas syringae pv. tomato DC3000 type III secretion effector genes reveal functional overlap among effectors. PLoS Pathog 5: e1000388
Google Scholar: Author Only Title Only Author and Title

Larsson J (2020) eulerr: Area-proportional euler and venn diagrams with ellipses. R package version 6.1.0. Available at: https://cran.r-project.org/package=eulerr.
Google Scholar: Author Only Title Only Author and Title

Lee S, Ishiga Y, Clermont K, Mysore KS (2013) Coronatine inhibits stomatal closure and delays hypersensitive response cell death induced by nonhost bacterial pathogens. PeerJ 1: e34
Google Scholar: Author Only Title Only Author and Title

Li L, Li M, Yu L, Zhou Z, Liang X, Liu Z, Cai G, Gao L, Zhang X, Wang Y, et al. (2014) The FLS2-associated kinase BIK1 directly phosphorylates the NADPH oxidase RbohD to control plant immunity. Cell Host Microbe 15: 329–338
Google Scholar: Author Only Title Only Author and Title

Li R, Liu P, Wan Y, Chen T, Wang Q, Mettbach U, Baluška F, Šamaj J, Fang X, Lucas WJ, et al. (2012a) A membrane microdomain-associated protein, Arabidopsis Flot1, is involved in a clathrin-independent endocytic pathway and is required for seedling development. Plant Cell 24: 2105–2122
Google Scholar: Author Only Title Only Author and Title

Li ZY, Xu ZS, He GY, Yang GX, Chen M, Li LC, Ma YZ (2012b) A mutation in Arabidopsis BSK5 encoding a brassinosteroid-signaling kinase protein affects responses to salinity and abscisic acid. Biochem Biophys Res Commun 426: 522–527
Google Scholar: Author Only Title Only Author and Title

Liang X, Zhou J-M (2018) Receptor-like cytoplasmic kinases: Central players in plant receptor kinase–mediated signaling. Annu Rev Plant Biol 69: 267–299
Google Scholar: Author Only Title Only Author and Title

Liu Y, Maierhofer T, Rybak K, Sklenar J, Breakspear A, Johnston MG, Fliegmann J, Huang S, Roelfsema MRG, Felix G, et al (2019) Anion channel SLAH3 is a regulatory target of chitin receptor-associated kinase PBL27 in microbial stomatal closure. Elife. 8: e44474
Google Scholar: Author Only Title Only Author and Title

Ma L, Salas O, Bowler K, Oren-Young L, Bar-Peled M, Sharon A (2017) Genetic alteration of UDP-rhamnose metabolism in Botrytis cinerea leads to the accumulation of UDP-KDG that adversely affects development and pathogenicity. Mol Plant Pathol 18: 263–275
Google Scholar: Author Only Title Only Author and Title

Ma SW, Morris, VL, Cuppels DA (1991) Characterization of a DNA region required for production of the phytotoxin coronatine by Pseudomonas syringae pv. tomato. Mol Plant-Microbe Interact 4: 69
Google Scholar: Author Only Title Only Author and Title

Majhi BB, Sobol G, Gachie S, Sreeramulu S, Sessa G (2021) BRASSINOSTEROID-SIGNALLING KINASES 7 and 8 associate with the FLS2 immune receptor and are required for flg22-induced PTI responses. Mol Plant Pathol 22: 786–799
Google Scholar: Author Only Title Only Author and Title

Majhi BB, Sreeramulu S, Sessa G (2019) BRASSINOSTEROID-SIGNALING KINASE5 associates with immune receptors and is required for immune responses. Plant Physiol 180: 1166–1184
Google Scholar: Author Only Title Only Author and Title

Melotto M, Underwood W, Koczan J, Nomura K, He SY (2006) Plant stomata function in innate immunity against bacterial invasion. Cell 126: 969–980
Google Scholar: Author Only Title Only Author and Title

Melotto M, Zhang L, Oblessuc PR, He SY (2017) Stomatal defense a decade later. Plant Physiol 174: 561–571
Google Scholar: Author Only Title Only Author and Title

Mortazavi A, Williams BA, McCue K, Schaeffer L, Wold B (2008) Mapping and quantifying mammalian transcriptomes by RNA-Seq. Nat Methods 5: 621–628
Google Scholar: Author Only Title Only Author and Title

Murray MG, Thompson WF (1980) Rapid isolation of high molecular weight plant DNA. Nucleic Acids Res 8: 4321–4326
Google Scholar: Author Only Title Only Author and Title

Ooms G, Hooykaas PJJ, Van Veen RJM, Van Beelen P, Regensburg-Tuïnk TJG, Schilperoort RA (1982) Octopine Ti-plasmid deletion mutants of Agrobacterium tumefaciens with emphasis on the right side of the T-region. Plasmid 7: 15–29
Google Scholar: Author Only Title Only Author and Title

Popov G, Fraiture M, Brunner F, Sessa G (2016) Multiple Xanthomonas euvesicatoria type III effectors inhibit flg22-triggered immunity. Mol Plant Microbe Interact 29: 651–660
Google Scholar: Author Only Title Only Author and Title

Rao S, Zhou Z, Miao P, Bi G, Hu M, Wu Y, Feng F, Zhang X, Zhou J-M (2018) Roles of receptor-like cytoplasmic kinase VII members in pattern-triggered immune signaling. Plant Physiol 177: 1679-1690
Google Scholar: Author Only Title Only Author and Title

Raudvere U, Kolberg L, Kuzmin I, Arak T, Adler P, Peterson H, Vilo J (2019) g:Profiler: a web server for functional enrichment analysis and conversions of gene lists (2019 update). Nucleic Acids Res 47: W191–W198
Google Scholar: Author Only Title Only Author and Title

Ren H, Willige BC, Jaillais Y, Geng S, Park MY, Gray WM, Chory J (2019) BRASSINOSTEROID-SIGNALING KINASE 3, a plasma

membrane-associated scaffold protein involved in early brassinosteroid signaling. PLOS Genet 15: e1007904
Google Scholar: Author Only Title Only Author and Title

Robatzek S, Bittel P, Chinchilla D, Köchner P, Felix G, Shiu S-H, Boller T (2007) Molecular identification and characterization of the tomato flagellin receptor LeFLS2, an orthologue of Arabidopsis FLS2 exhibiting characteristically different perception specificities. Plant Mol Biol 64: 539–47
Google Scholar: Author Only Title Only Author and Title

Roberts R, Hind SR, Pedley KF, Diner BA, Szarzanowicz MJ, Luciano-Rosario D, Majhi BB, Popov G, Sessa G, Oh C-S, et al. (2019a) Mai1 protein acts between host recognition of pathogen effectors and mitogen-activated protein kinase signaling. Mol Plant-Microbe Interact 32: 1496–1507
Google Scholar: Author Only Title Only Author and Title

Roberts R, Mainiero S, Powell AF, Liu AE, Shi K, Hind SR, Strickler SR, Collmer A, Martin GB (2019b) Natural variation for unusual host responses and flagellin-mediated immunity against Pseudomonas syringae in genetically diverse tomato accessions. New Phytol 223: 447–461
Google Scholar: Author Only Title Only Author and Title

Roberts R, Liu AE, Wan L, Geiger AM, Hind SR, Rosli HG, Martin GB (2020) Molecular characterization of differences between the tomato immune receptors Flagellin sensing 3 and Flagellin sensing 2. Plant Physiol 183: 1825–1837
Google Scholar: Author Only Title Only Author and Title

Rosli HG, Zheng Y, Pombo MA, Zhong S, Bombarely A, Fei Z, Collmer A, Martin GB (2013) Transcriptomics-based screen for genes induced by flagellin and repressed by pathogen effectors identifies a cell wall-associated kinase involved in plant immunity. Genome Biol 14: 1-15
Google Scholar: Author Only Title Only Author and Title

Salomon D, Sessa G (2010) Identification of growth inhibition phenotypes induced by expression of bacterial type III effectors in yeast. J Vis Exp. 37: e1865
Google Scholar: Author Only Title Only Author and Title

Sasaki-Sekimoto Y, Jikumaru Y, Obayashi T, Saito H, Masuda S, Kamiya Y, Ohta H, Shirasu K (2013) Basic helix-loop-helix transcription factors JASMONATE-ASSOCIATED MYC2-LIKE1 (JAM1), JAM2, and JAM3 are negative regulators of jasmonate responses in arabidopsis. Plant Physiol 163: 291–304
Google Scholar: Author Only Title Only Author and Title

Shi H, Li Q, Luo M, Yan H, Xie B, Li X, Zhong G, Chen D, Tang D (2022) BRASSINOSTEROID-SIGNALING KINASE1 modulates MAP KINASE15 phosphorylation to confer powdery mildew resistance in Arabidopsis. Plant Cell.
Google Scholar: Author Only Title Only Author and Title

Shi H, Shen Q, Qi Y, Yan H, Nie H, Chen Y, Zhao T, Katagiri F, Tang D (2013) BR-SIGNALING KINASE1 physically associates with FLAGELLIN SENSING2 and regulates plant innate immunity in Arabidopsis. Plant Cell 25: 1143–1157
Google Scholar: Author Only Title Only Author and Title

Sierla M, Waszczak C, Vahisalu T, Kangasjärvi J (2016) Reactive oxygen species in the regulation of stomatal movements. Plant Physiol 171: 1569–1580
Google Scholar: Author Only Title Only Author and Title

Singh DK, Calviño M, Brauer EK, Fernandez-Pozo N, Strickler S, Yalamanchili R, Suzuki H, Aoki K, Shibata D, Stratmann JW, et al. (2014) The tomato kinome and the tomato kinase library ORFeome: Novel resources for the study of kinases and signal transduction in tomato and Solanaceae species. Mol Plant-Microbe Interact 27: 7–17
Google Scholar: Author Only Title Only Author and Title

Smirnova E, Marquis V, Poirier L, Aubert Y, Zumsteg J, Ménard R, Miesch L, Heitz T (2017) Jasmonic Acid Oxidase 2 hydroxylates jasmonic acid and represses basal defense and resistance responses against Botrytis cinerea infection. Mol Plant 10: 1159–1173
Google Scholar: Author Only Title Only Author and Title

Sreeramulu S, Mostizky Y, Sunitha S, Shani E, Nahum H, Salomon D, Hayun L Ben, Gruetter C, Rauh D, Ori N, et al. (2013) BSKs are partially redundant positive regulators of brassinosteroid signaling in Arabidopsis. Plant J 74: 905–919
Google Scholar: Author Only Title Only Author and Title

Su B, Wang A, Shan X (2022) The role of N-myristoylation in homeostasis of brassinosteroid signaling kinase 1. Planta 255: 73
Google Scholar: Author Only Title Only Author and Title

Su B, Zhang X, Li L, Abbas S, Yu M, Cui Y, Baluška F, Hwang I, Shan X, Lin J (2021) Dynamic spatial reorganization of BSK1 complexes in the plasma membrane underpins signal-specific activation for growth and immunity. Mol Plant 14: 588–603
Google Scholar: Author Only Title Only Author and Title

Tang W, Kim T-W, Oses-Prieto JA, Sun Y, Deng Z, Zhu S, Wang R, Burlingame AL, Wang Z-Y (2008) BSKs mediate signal transduction from the receptor kinase BRI1 in Arabidopsis. Science 321: 557–60

Google Scholar: Author Only Title Only Author and Title

Thaler JS, Humphrey PT, Whiteman NK (2012) Evolution of jasmonate and salicylate signal crosstalk. Trends Plant Sci 17: 260–270
Google Scholar: Author Only Title Only Author and Title

Thor K, Jiang S, Michard E, George J, Scherzer S, Huang S, Dindas J, Derbyshire P, Leitão N, DeFalco TA, et al (2020) The calcium-permeable channel OSCA1.3 regulates plant stomatal immunity. Nature 585: 569–573
Google Scholar: Author Only Title Only Author and Title

Tian W, Hou C, Ren Z, Wang C, Zhao F, Dahlbeck D, Hu S, Zhang L, Niu Q, Li L, et al (2019) A calmodulin-gated calcium channel links pathogen patterns to plant immunity. Nature 572: 131–135
Google Scholar: Author Only Title Only Author and Title

Tomato Genome Consortium (2012) The tomato genome sequence provides insights into fleshy fruit evolution. Nature 485: 635–641
Google Scholar: Author Only Title Only Author and Title

Toum L, Torres PS, Gallego SM, Benavídes MP, Vojnov AA, Gudesblat GE (2016) Coronatine inhibits stomatal closure through guard cell-specific inhibition of NADPH oxidase-dependent ROS production. Front Plant Sci. 1851
Google Scholar: Author Only Title Only Author and Title

Vanholme R, De Meester B, Ralph J, Boerjan W (2019) Lignin biosynthesis and its integration into metabolism. Curr Opin Biotechnol 56: 230-239.
Google Scholar: Author Only Title Only Author and Title

Wang H, Hutton SF, Robbins MD, Sim S-C, Scott JW, Yang W, Jones JB, Francis DM (2011) Molecular mapping of hypersensitive resistance from tomato 'Hawaii 7981' to Xanthomonas perforans race T3. Phytopathology 101: 1217–1223
Google Scholar: Author Only Title Only Author and Title

Wang L, Albert M, Einig E, Fürst U, Krust D, Felix G (2016) The pattern-recognition receptor CORE of Solanaceae detects bacterial cold-shock protein. Nat Plants 2: 16185
Google Scholar: Author Only Title Only Author and Title

Wang Z, Gou X (2021) The first line of defense: Receptor-like protein kinase-mediated stomatal immunity. Int J Mol Sci 23: 343
Google Scholar: Author Only Title Only Author and Title

Wasternack C, Song S (2016) Jasmonates: biosynthesis, metabolism, and signaling by proteins activating and repressing transciption. J Exp Bot 68: 1303-1321
Google Scholar: Author Only Title Only Author and Title

Weyers JDB, Johansen LG (1985) Accurate estimation of stomatal aperture from silicone rubber impressions. New Phytol 101: 109–115
Google Scholar: Author Only Title Only Author and Title

Wilson M, Campbell HL, Ji P, Jones JB, Cuppels DA (2002) Biological control of bacterial speck of tomato under field conditions at several locations in north america. Phytopathology 92: 1284–1292
Google Scholar: Author Only Title Only Author and Title

Xing Y (2006) An expectation-maximization algorithm for probabilistic reconstructions of full-length isoforms from splice graphs. Nucleic Acids Res 34: 3150–3160
Google Scholar: Author Only Title Only Author and Title

Xu P, Xu S-L, Li Z-J, Tang W, Burlingame AL, Wang Z-Y (2014) A brassinosteroid-signaling kinase interacts with multiple receptor-like kinases in Arabidopsis. Mol Plant 7: 441–444
Google Scholar: Author Only Title Only Author and Title

Yan H, Zhao Y, Shi H, Li J, Wang Y, Tang D (2018) BRASSINOSTEROID-SIGNALING KINASE1 phosphorylates MAPKKK5 to regulate immunity in Arabidopsis. Plant Physiol 176: 2991-3002
Google Scholar: Author Only Title Only Author and Title

Yi SY, Shirasu K, Moon JS, Lee S-G, Kwon S-Y (2014) The activated SA and JA signaling pathways have an influence on flg22-triggered oxidative burst and callose deposition. PLoS One 9: e88951
Google Scholar: Author Only Title Only Author and Title

Zhang L, Zhang F, Melotto M, Yao J, He SY (2017) Jasmonate signaling and manipulation by pathogens and insects. J Exp Bot 68: 1371-1385
Google Scholar: Author Only Title Only Author and Title

Zhang N, Pombo MA, Rosli HG, Martin GB (2020) Tomato wall-associated kinase SlWak1 depends on Fls2/Fls3 to promote apoplastic immune responses to Pseudomonas syringae. Plant Physiol 183: 1869–1882
Google Scholar: Author Only Title Only Author and Title

Zheng X, Kang S, Jing Y, Ren Z, Li L, Zhou J-M, Berkowitz G, Shi J, Fu A, Lan W, et al (2018) Danger-associated peptides close stomata by OST1-independent activation of anion channels in guard cells. Plant Cell 30: 1132–1146

Google Scholar: Author Only Title Only Author and Title

Zheng X, Spivey NW, Zeng W, Liu P-P, Fu ZQ, Klessig DF, He SY, Dong X (2012) Coronatine promotes Pseudomonas syringae virulence in plants by activating a signaling cascade that inhibits salicylic acid accumulation. Cell Host Microbe 11: 587–596

Google Scholar: Author Only Title Only Author and Title

Zipfel C, Robatzek S, Navarro L, Oakeley EJ, Jones JDG, Felix G, Boller T (2004) Bacterial disease resistance in Arabidopsis through flagellin perception. Nature 428: 764–767

Google Scholar: Author Only Title Only Author and Title